THE ROLE OF LIPASE MATURATION FACTOR 1 IN THE MATURATION OF LIPOPROTEIN LIPASE

Melissa A. Babilonia-Rosa

A dissertation submitted to the faculty at the University of North Carolina at Chapel Hill in partial fulfillment of the requirements for the degree of Doctor of Philosophy in the Department of Biochemistry and Biophysics.

Chapel Hill
2016

Approved by:

Saskia Neher

Henrik Dohlman

Brian Kuhlman

Rosalind Coleman

Amy Shaub Maddox

© 2016
Melissa A. Babilonia-Rosa
ALL RIGHTS RESERVED

ABSTRACT

Melissa A. Babilonia-Rosa: The Role of Lipase Maturation Factor 1 in the Maturation of Lipoprotein Lipase
(Under the direction of Saskia Neher)

Over a third of the US adult population has elevated blood triglyceride (TG) levels (hypertriglyceridemia), resulting in an increased risk of atherosclerosis, pancreatitis, and metabolic syndrome. Lipases are responsible for lipid uptake from dietary sources and for the distribution of fatty acids to different tissues. Lipoprotein lipase (LPL), a dimeric enzyme, is the main lipase responsible for TG clearance from the blood after food intake. In difference of monomeric lipases, dimeric lipases require lipase maturation factor 1 (LMF1) for proper folding, activity, and secretion. LMF1 is a transmembrane protein located in the endoplasmic reticulum (ER). Although LMF1 is crucial for ER exit of dimeric lipases, the mechanism by which LMF1 promotes lipase maturation is not known. *My thesis work aims to understand LMF1's role in LPL maturation using cell biology and biochemical methods.* I have developed N-terminal truncation mutants of LMF1, which revealed that full length LMF1 is required for the maturation of LPL. We employed LMF1-crosslinking/mass spectrometry studies to identify proteins with a role in LPL maturation. Our novel interacting partners of LMF1 and LPL were validated by pull down assays and by protein knockdowns to assess effects on LPL maturation.

We found five novel, ER-resident binding partners of LMF1. Three of these proteins are involved in formation and isomerization of disulfide bonds. Given the role in oxidative folding of most of the new partners we propose that LMF1 promotes LPL folding by promoting redox homeostasis in the ER.

ACKNOWLEDGEMENTS

I started graduate school at UNC looking for career development and I am happy to say that I am headed to a slightly different path than I initially thought because I discovered something new and exciting for me. During the past six years a lot of people have helped me attain my goals and I am grateful for the time they allotted to my training and for their support. First and foremost, I would like to thank my Ph.D. advisor Dr. Saskia Neher. Her continuous guidance was instrumental to my improvement and development as a research scientist. I am also thankful for Dr. Neher's support through my teaching internship at UNC. In addition to my advisor, I would like to thank the rest of my thesis committee: Drs. Henrik Dohlman, Brian Kuhlman, Amy Shaub Maddox, and Rosalind Coleman. Thank you for your guidance through troubleshooting and making sure I had the appropriate controls. Additionally, our continued questions forced me to broaden my understanding of not only my own work but of other biochemical processes.

I am also thankful to past and present members of the Neher laboratory that have helped me complete this journey. Lindsey Broadwell has been an exceptional undergraduate during the past year. Most significantly, I injured my hand through repetitive motions collecting samples to wrap up my thesis and Lindsey was of great help finishing the last experiments under my guidance. Christopher (Brian) Garrett, Cassandra Hayne, and Melissa Ritchie were supportive of my happy fruitful science days as well as the not so good science days.

I am thankful to the Microscopy Services Laboratory, especially to Pablo Ariel

and Robert Bagnell for teaching me about microscopy and data analysis. Additionally, Stephanie Gupton, Courtney Winkle, and Benjamin Roberts (from the Neher laboratory) helped with co-localization data analysis.

Special thanks to the current and past members of the Office of Graduate Education: Joshua Hall, Patrick Brandt, Ashalla Freeman, Jessica Harrell, Rebekah Layton, and Erin Hopper. They have all supported different aspects of my career throughout my years in graduate school but I would like to thank Josh and Patrick for the opportunity to travel twice to Puerto Rico to gain teaching experience by giving science workshops at the UPR-Humacao while recruiting undergraduate students to different programs at UNC. Beka gave me the opportunity to be one of the founders and chairs of Future Science Educators or FuSE, a cohort for graduate students and post-doctoral fellows interested in teaching intensive careers. Lastly, Ashalla for doing a spectacular job of maintaining a community of minority students on campus that supports each other through scientific and social events.

Lastly, I am grateful for my support group outside of graduate school. I would like to thank Greg Palczewski and Ivy Babilonia for their continued support, especially in high stress periods. I also thank my family especially Mayra and Nelly Rosa. Your support before and during graduate school helped me develop into who I am today.

TABLE OF CONTENTS

LIST OF TABLES

LIST OF FIGURES

LIST OF ABBREVIATIONS

aa	amino acid
ANGPTL	angiopoietin-like proteins
Apo	apolipoproteins
cld	combined lipase deficiency
CM	chylomicron
DMEM	Dubelcco's modified eagle medium
DSP	dithiobis-succinimidyl propionate
DUF1222	domain of unknown function 1222
EL	endothelial lipase
ER	endoplasmic reticulum
ERdj5	endopasmic reditculum resident protein ERdj5
ERAD	endoplasmic reticulum associated degradation
ERp44	endoplasmic reticulum resident protein 44
ERp72	endoplasmic reticulum resident protein 72
FBS	fetal bovine serum
FL	full length
GAPDH	glyceraldehyde-3-phosphate dehydrogenase
GPIHBP1	glycosylphosphatidylinositol anchored high-density lipoprotein binding protein 1
HDL	high-density lipoprotein
HL	hepatic lipase
IDL	intermediate-density lipoprotein
LDL	low-density lipoprotein

LMF1	lipase maturation factor 1
LPL	lipoprotein lipase
MEF	mouse embryonic fibroblasts
NEM	N-Ethylmaleimide
pBpa	*p* –benzoylphenylalanine
PDI	protein disulfide isomerase
PL	pancreatic lipase
PPA	protease protection assay
PR	progesterone receptor
SDS-PAGE	sodium dodecyl sulfate-polyacrylamide gel electrophoresis
TCA	trichloroacetic acid
TG	triglyceride
TXNIP	thioredoxin-interacting protein
TRX	thioredoxin
UGGT1	glycoprotein glucosyltransferase 1
UGGT2	glycoprotein glucosyltransferase 2
VLDL	very low-density lipoprotein
WT	wild type

CHAPTER 1: INTRODUCTION

The lipase gene family

Lipases are hydrolases present in organisms ranging from prokaryotes to humans that mediate the absorption, transport, storage, and mobilization of lipids. Here, we focus on the dimeric lipases lipoprotein lipase (LPL), hepatic lipase (HL), and endothelial lipase (EL). These three lipases belong to the same gene family[1,2]. They reside in the capillary lumen, anchored to the endothelial lining where they hydrolyze lipids from lipoproteins, releasing fatty acids that can be absorbed by neighboring tissue for triglyceride (TG) and phospholipid clearance from the plasma. The three lipases differ in the tissues in which they are expressed and in their substrate specificity. LPL is mainly expressed in the heart, adipose tissue, and skeletal muscle but mRNA expression has been reported in the brain, lung, adrenal gland, and placenta[3-5]. LPL activity has been detected in heart, adipocytes, muscle, lungs, kidney and brain[6]. HL is synthetized mainly in the liver but its also expressed in macrophages[7]. In contrast to LPL and HL which are expressed in different cell types but active at the endothelial lining of the capillary lumen, EL is synthetized by endothelial cells and northern-blot analysis across different human tissues show mRNA expression in the lungs, liver, placenta, and kidneys[4]. In terms of substrate specificity, LPL primarily hydrolyzes TG, EL is primarily a phospholipase, and HL can hydrolyze both substrates[8].

Pancreatic lipase (PL) is another member of the lipase gene family and it resides in the intestines where it hydrolyzes TG from dietary fats. Phylogenic analysis of the

lipase gene family suggests that PL diverged from an ancestral lipase previous to the dimeric lipases[1,9]. EL was the last lipase member to be identified; its primary sequence is 45% homologous to LPL, 40% homologous to HL, and 27% homologous to PL[4]. A combination of site directed mutagenesis and computational studies have revealed these lipases share an active serine site within a characteristic pentapeptide sequence GXSXG[10-13]. In addition to sequence similarity, these four lipases share structural features. PL is the only one of these lipases with a known structure[14]. Computational modeling studies based on crystal structures of PL from horse, porcine, and human[14-17] suggest that EL, LPL, and HL contain an N-terminal domain that is responsible for their catalytic activity. The N-terminal domain harbors a (Ser-Asp-His) catalytic triad with a α/β hydrolase fold[13,18] (**Fig. 1.1**). The N-terminus also harbors the lid, which confers substrate specificity and covers the catalytic site in the closed conformation preventing substrate hydrolysis. Activity studies performed with chimeras comprised of LPL's body and HL's lid, or HL's body and LPL's lid, reveal that lid exchange is sufficient to change the substrate specificity of the LPL chimera from TG to phospholipids whereas the HL chimera gains specificity towards phospholipids[19]. The lid contains an amphipathic helix-turn-helix motif that is important for the physiological function of LPL and HL as revealed by site-directed mutagenesis studies[20]. This study also revealed that replacing the 22 amino acid lid of LPL with a shorter lid of 4 amino acids enhances hydrolysis of a short chain TG substrate such as tributyrin but abolishes hydrolysis of a long chain TG substrate like triolein. The C-terminal domain has a β-sandwich fold which contains a heparin binding site for LPL and HL. Additionally, a tryptophan cluster in the C-terminus of LPL is important for substrate recognition[18,21].

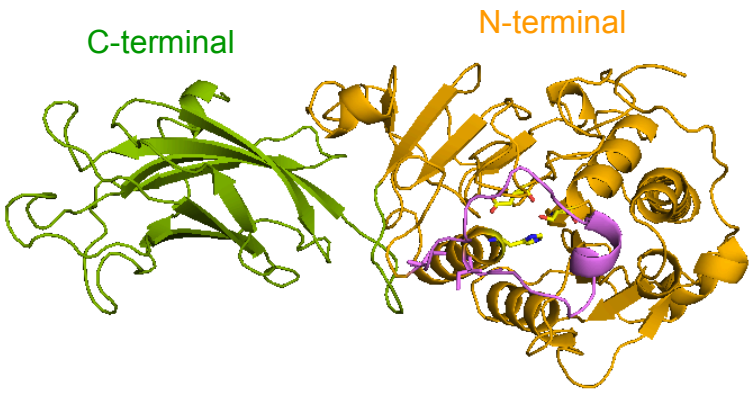

Figure 1.1 Model of an LPL monomer.
I-TASSER[22] was used to obtain a predicted 3D structure of human LPL. The catalytic triad (Ser132 - Asp156 - His241) is shown in yellow. The lid covering the catalytic triad is shown in magenta with the stick representation of disulfide bond at the end of the lid. Michael Lafferty generated this model based on sequence similarity to pancreatic lipase.

Lipoproteins are important for the transport of TGs within the capillary lumen. They consist of a hydrophobic core of TGs and cholesteryl esters, and a hydrophilic surface that consists of phospholipids, cholesterol, and proteins known as apolipoproteins[23,24]. There are five types of lipoproteins synthetized in different tissues and categorized according to particle density; a property that changes with lipid and protein composition (**Fig. 1.2A**). Chylomicrons (CM) are the most buoyant lipoproteins as they have the most TGs in their core. They are synthesized in the small intestines by enterocytes from re-esterified fatty acids generated from the hydrolysis of dietary TGs by PL. Newly synthesized CMs enter the capillary lumen through the lymphatic system to deliver TG to peripheral tissues (**Fig. 1.2B**). Very-low density lipoprotein (VLDL) is the lipoprotein with the second highest TG content. The liver secretes VLDL to redistribute TG to adipose, heart, and muscle tissue. Upon TG hydrolysis by LPL in the capillary lumen, the TG content of CM and VLDL decreases by ~90% generating lipoproteins[25] of higher density. Chylomicrons are released to the capillary lumen in the fed state whereas VLDL is secreted upon fasting. CM are transformed into CM remnants and VLDL is transformed to intermediate-density lipoprotein (IDL) and subsequently to low-density lipoprotein (LDL). High-density lipoprotein (HDL) is critical for reverse cholesterol transport as it moves cholesterol from peripheral tissues to the liver.

Substrate specificity of the lipases expressed at the capillary lumen allows for different lipoprotein preference and in consequence, the role of these lipases in lipoprotein metabolism varies. LPL hydrolyzes CM and VLDL (**Fig. 1.2B**), thus there is an accumulation of these lipoproteins in humans with LPL deficiency[26,27]. Conversely, LPL overexpression in mice results in decreased levels of plasma TG[28]. HL converts

IDL to LDL and post-prandial TG-rich HDL into TG-poor HDL[29]. Thus HL knockout mice have elevated total cholesterol and HDL cholesterol while TG levels remain comparable to WT mice (mice display only mild dyslipidemia following targeted inactivation of the hepatic lipase gene). Lastly, EL is primarily a phospholipase; hence it hydrolyzes phospholipids in HDL. As a result, EL overexpression in mice lowers HDL levels and mice knockouts have higher HDL levels when compared to control mice[30].

A.

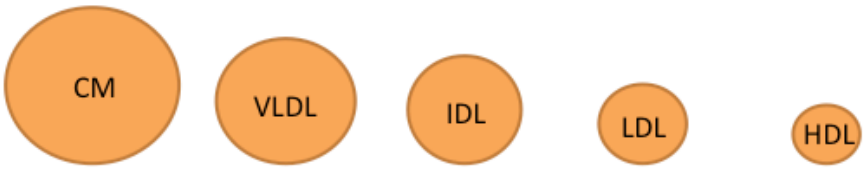

Density (g/ml)	<0.960	0.960-1.006	1.006-1.019	1.019-1.063	1.063-1.210
Cholesterol (%)	4	23	43	58	41-35
TG (%)	88	56	29	13	16-13
Protein (%)	1	8	11	21	33-57

B.

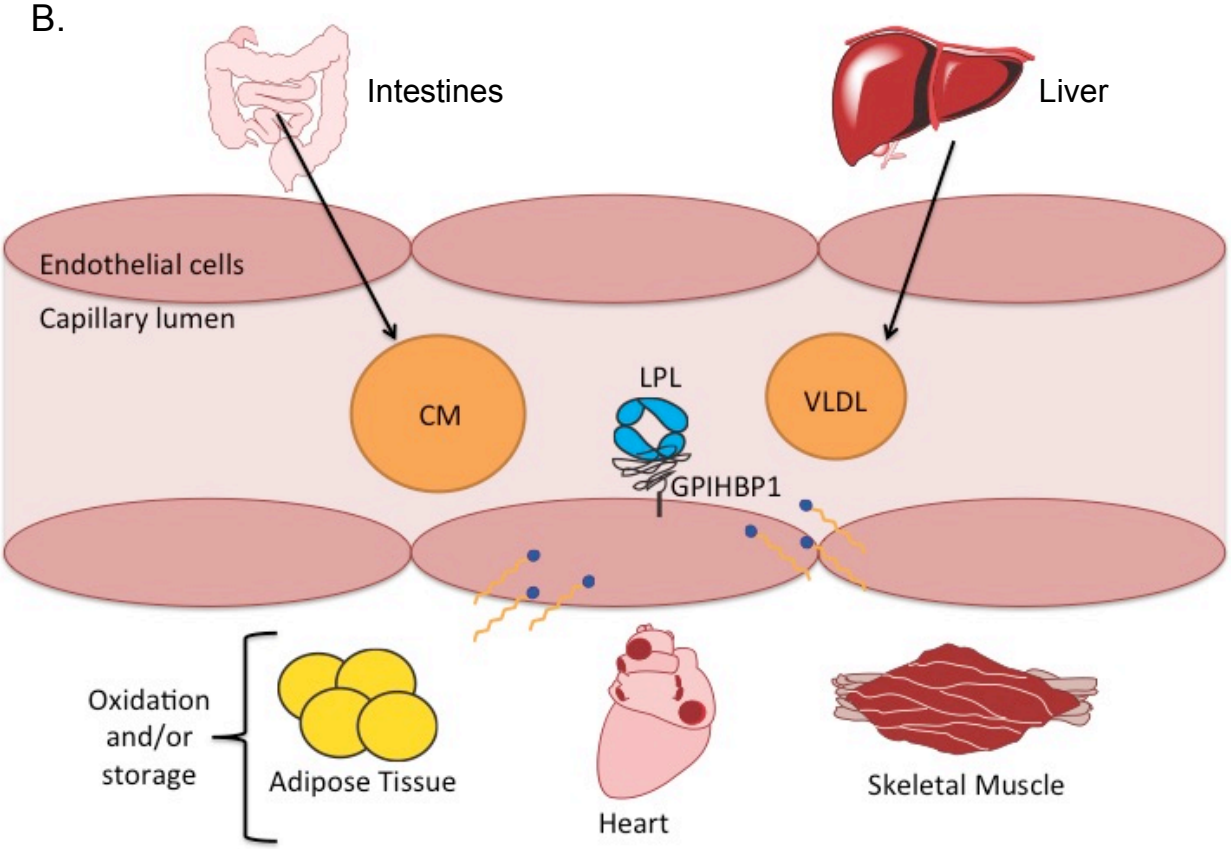

Figure 1.2 Role of lipoproteins and LPL in TG transport in the capillary lumen. A) Characteristics of lipoproteins as modified from Biggerstaff *et. al.* 2004. The orange cartoons are a visual representation of the particle size. B) CM and VLDL are TG dense lipoproteins synthetized in the small intestines and liver, respectively. Both of these lipoproteins are secreted into the capillary lumen where they interact with LPL for TG hydrolysis. The fatty acids released are used for energy production or storage in adipocytes, heart, and muscle.

Regulation of LPL activity by interacting proteins

LPL is the rate-limiting enzyme for the hydrolysis of TG within the capillary lumen. LPL activity rises in white adipose tissue (WAT) after feeding while it declines in the heart and muscle; this leads to TG storage in adipocytes. The opposite effect is seen during fasting, LPL activity in the muscle and heart increases where the released fatty acids are used for storage or oxidized to generate energy. LPL within the capillary lumen is regulated by interacting partners such as apolipoproteins, angiopoietin-like proteins, and glycosylphosphatidylinositol-anchored high-density lipoprotein binding protein 1 (GPIHBP1).

Plasma lipoproteins contain apolipoproteins that interact with LPL and modulate its activity. Apolipoprotein C-II (ApoCII) and AV (ApoAV) are known to promote LPL activity whereas ApoCI and CIII inhibit LPL[31]. ApoCII is mainly synthesized in the liver and it is a 79 amino acid peptide constituent of CM, VLDL, LPL and HDL[32]. *In vitro* activity assays with LPL purified from rat and ApoCII purified from VLDL or HDL revealed that ApoCII is a cofactor for LPL[33]. Furthermore, individuals with mutations in ApoCII accumulate TGs in the plasma because LPL needs ApoCII for efficient CM and VLDL hydrolysis[34,35]. The N-terminal domain of ApoCII contains the lipid-binding domain and the C-terminal domain interacts with LPL[35]. Crosslinking experiments of ApoCII with bovine LPL revealed a region of 11 amino acids in the N-terminus of ApoCII that bind to LPL[36].

ApoCI and CIII are mainly synthesized in the liver and they associate with CM, VLDL, and HDL[37]. Overexpression of either ApoCI or CIII in mice promotes an increase in TG levels[38,39]. Similarly, mice knockouts CIII have reduced plasma TG levels and

APOCIII loss of function mutations in humans are associated with reduced TG levels and reduced risk for coronary heart disease[40-42]. However, ApoCI knockout mice only show a trend towards lower TG levels and it seems that ApoCI impairs the binding of VLDL to the VLDL receptor thus resulting in VLDL accumulation in mice overexpressing ApoCI[43]. Another possible explanation for the inhibition of LPL activity by this apolipoproteins is LPL displacement from the lipoproteins[44]. Due to the discrepancy between *in vitro* and *in vivo* studies, further studies are needed to clarify the roles of ApoC1 and CIII in TG metabolism.

ApoAV is also predominantly expressed in the liver and it associates with VLDL and HDL[45]. Transgenic mice overexpressing ApoAV have a 66% reduction in TG levels while mice knockouts display a 4-fold increase in TG levels when compared to controls[46]. Supporting the involvement of ApoAV in TG metabolism, loss of function mutations in humans lead to severe hypertriglyceridemia[47,48]. Two *in vitro* studies support the hypothesis that ApoA5 increases LPL activity[45]. Recombinant ApoAV stimulates LPL activity: 1) with addition of ApoCII and 2) with addition of VLDL isolated from mouse plasma. However, other *in vitro* studies do not support the hypothesis of ApoAV as an LPL activator. The conflicting data might result from utilization of different substrates. Other modes of action proposed for ApoAV have been intracellular repression of VLDL synthesis or activation of receptor mediated lipoprotein endocytosis in the liver[31]. Further studies are necessary to further understand the role of ApoAV in TG metabolism.

The angiopoietin-like protein (ANGPTL) family is comprised of eight secreted proteins[49]. With the exception of ANGPTL8, family members have an N-terminal coiled-

coil domain and a C-terminal fibrinogen like domain. Three family members, ANGPTL3, 4 and 8, are known to alter TG metabolism by inhibition of LPL's activity. ANGPTL3 and 4 are cleaved by protein convertases like FURIN releasing the N-terminal domain, which inhibits LPL. This cleavage is crucial for LPL inhibition. ANGPTL4 functions as a homo-oligomer and studies from our lab have revealed that ANGPTL4 is a reversible inhibitor of LPL[50]. ANGPTL8 lacks the C-terminal domain characteristic of the family but the N-terminal domain still shares 20% sequence identity with ANGPTL3 and 4, suggesting similar functions[51]. This region includes the ~25 residues of ANGPTL3 and 4 known to bind LPL[52]. Adenoviral expression of ANGPTL8 in mice liver results in increased plasma TG levels whereas co-expression of ANGPTL8 and 3 further exacerbate TG accumulation; expression of ANGPTL3 alone does not alter TG levels[53]. Additionally, co-immunoprecipitation studies from plasma of these mice show that ANGPTL8 interacts with the N-terminal domain of ANGPTL3. Lastly, the N-terminal domain of ANGPTL3 is released into the media of hepatocytes co-expressing ANGPTL8 and 3 whereas cells expressing only ANGPTL3 release full-length protein. Taken together, these findings suggest that ANGPTL8 inhibits LPL in an ANGPTL3-dependent manner.

ANGPTL3, 4, and 8 mediate LPL inhibition but they do so in different tissues and at different times in the fed-fasting cycle[54]. ANGPTL4 inhibits LPL in WAT while ANGPTL4 and 8 work in the heart and skeletal muscle. Fasting upregulates ANGPTL4, which downregulates LPL's activity in adipose tissue. Conversely, fasting downregulates ANGPTL8 so LPL remains active in the heart and muscle. As a result, during fasting, LPL in the heart and muscle hydrolyzes TG from chylomicrons and VLDL

providing fatty acids to be oxidized for energy. After a meal, ANGPTL4 is downregulated while ANGPTL8 is upregulated. In consequence, LPL remains active in WAT and inactive in the heart/muscle.

The mechanism by which LPL reaches the capillary lumen remained a mystery until GPIHBP1 was discovered in 2010[55]. Immunohistochemical studies with a fluorescently labeled antibody against GPIHBP1 revealed that GPIHBP1 is expressed in the capillary lumen in tissues from WT mice. In WT mice, LPL co-localizes with the GPIHBP1 and can travel to its site of action in the capillary lumen of these tissues. In mice lacking GPIHBP1, LPL becomes stuck in the interstitial spaces surrounding myocytes and adipocytes. This finding explains why GPIHBP1 deficient mice have severe hypertriglyceridemia[56]; LPL is not transported to the capillary lumen for hydrolysis of chylomicrons and VLDL. Confirmation of the role of GPIHBP1 in transport came from transwell assays using rat heart microvessel endothelial cells expressing GPIHBP1[57]. When LPL is added to the basolateral chamber of the transwells, it is translocated to the apical chamber only in the presence of GPIHBP1. The acidic domain of GPIHBP1 is known to bind LPL[58]. A final transwell experiment confirmed that GPIHPB1 with a mutation in the acidic domain is not capable of translocating LPL to the apical surface of endothelial cells. Lastly, the fact that GPIHBP1 does not bind HL, EL or PL was demonstrated by expression of GPIHBP1 followed by addition of conditioned media containing each of the lipases separately[59]. Immunofluorescence experiments confirmed that only LPL binds to cells expressing GPIHBP1.

Post-translational modifications of LPL

In order for LPL to be secreted in its active dimeric form, necessary post-translational modifications include subunit assembly, glycosylation, and disulfide bond formation[60]. LPL is active as a noncovalent homodimer in a head to tail subunit arrangement[61,62]. Similarly, HL and EL are also homodimers with a head to tail orientation[63,64] while PL is active as a monomer[65]. Dimerization of LPL, HL, and EL occurs in the ER where two populations of lipases can be found: 1) aggregated monomers that are inactive and eventually degraded and 2) active dimers that can exit the ER[66,67].

Like other glycosylated proteins[68], members of the lipase gene family contain a glycan chain covalently attached to the consensus sequence Asn-X-Ser/Thr. Asparagine mutations at positions 43, 56, and 62 of LPL, HL, and EL respectively, result in missfolding defects leading to ER retention and abolishment of lipase activity[69-71].

Sequence alignment of PL, LPL, HL, and EL shows these lipases share ten cysteines that are conserved across species[1,4] suggesting these residues have a role in the structure and function of these lipases. Disulfide bond pairing was determined sequencing disulfide linked tryptic peptides confirming the formation of 5 disulfide bonds[72]. Site directed mutagenesis of eight conserved cysteines demonstrates that six of the cysteines are critical for LPL activity[73]. The first conserved cysteine pair, C216/C239 for LPL, forms a disulfide bond in the lid of PL[62,74] where it is important for the opening and closing movement of the lid thus is important for substrate hydrolysis. The other two other disulfide pairs important for LPL activity are C264/C275 and C278/C283. The disulfide bond in the C-terminus of LPL, C418/C438, retains 85% of

activity when compared to WT. However, C418 is important for interaction with GPIHBP1 although disulfide bond formation is not required for the interaction[75]. In agreement with these findings, individuals with the C418Y LPL mutant have severe hypertriglyceridemia[76].

LMF1 is necessary for secretion of dimeric lipases

The relationship between dimeric lipases and lipase maturation factor 1 (LMF1) was discovered in 1983 in mice with an autosomal recessive mutation named combined lipase deficiency (cld)[77]. Mice homozygous for the *cld* mutation (*cld/cld)* appear normal at birth but they die within 48 hrs postpartum due to progressive triglyceride accumulation. However, heterozygous littermates (*cld/wt*) do not share this phenotype. Activity measurements of LPL and HL from heterozygous vs. homozygous *cld* mice revealed diminished lipase activity; subsequently impairment of EL activity was also demonstrated[9]. To understand why lipase activity levels are diminished in the plasma of *cld/cld* mice, mRNA levels of LPL and HL were measured from heart and liver and compared to heterozygous littermates[78]. Because mRNA levels are comparable for homozygous and heterozygous mice, the *cld* mutation was thought to affect protein synthesis or post-translational modifications. Pulse-chase experiments in heart and liver slices demonstrate that the rate of [^{35}S] methionine incorporation was slightly slower when comparing homozygous and heterozygous mice. However, *cld/cld* mice also showed lower rates of overall protein synthesis as well which seemed to be a result of the inability of these mice to use dietary triglycerides[78]. The next step to determine if the *cld* mutation affected lipase processing was Endo H digestion. N-linked glycoproteins like LPL and HL are glycosylated by oligosaccharyltransferase, which transfers high

mannose oligosaccharides as proteins emerge from the translocon. In the Golgi, high mannose units are removed and replaced by more complex sugars that are resistant to Endo H cleavage. As a result, Endo H treatment is used to probe accessibility of mannose units, which is correlated to the location of the glycosylated protein in the secretory pathway. Glycosylated proteins that have moved past the medial/trans-Golgi compartment are Endo H resistant whereas glycosylated proteins in the ER are Endo H sensitive[79]. Endo H treatment of liver immunoprecipitated LPL revealed that *cld/cld* mice only have LPL sensitive to Endo H. Thus LPL in these mice does not make it to the medial/trans-Golgi. However, LPL in the *cld/+* mice is both Endo H sensitive and resistant, representing protein being processed in the ER (Endo H sensitive) and protein that has entered the secretory pathway (Endo H resistant). Similarly, HL immunoprecipitations from homozygous and heterozygous livers followed by Endo H treatment reveal that HL also has a secretion defect in *cld/cld* mice; all the HL is Endo H sensitive[78]. Thus mRNA and protein levels of LPL and HL in *cld* mice are not affected but newly synthetized protein is retained in the ER, preventing Golgi processing and lipase secretion. However, Endo H testing of a different glycoprotein demonstrated that the *cld* mutation does not affect all N-linked glycoproteins thus the *cld* mutation does not confer a global failure in the glycosylation pathway[78].

Even though the *cld* mutation was discovered in 1983, the characterization of the gene responsible for the *cld* mutation was delayed over two decades. The *cld* mutation mapped to *t* haplotypes in Chromosome 17; a chromosomal region that contains four blocks of inversions that were challenging to map because recombination suppression prevented classical mapping approaches[77,80]. Genetic crosses between complementing

t haplotypes were key to remove early acting lethal mutations and avoid recombination suppression. These studies revealed that the *cld* mutation localizes to the haplotype t^{w73}, a region containing 149 genes. Genes to be tested were narrowed down by two methods. First, preference was given to genes involved protein folding or protein retention in the ER because it was known from the Endo H studies that LPL and HL in *cld/cld* mice does not move to the medial/trans-Golgi. Second, preference was given to genes demonstrating lower mRNA levels in homozygous vs. heterozygous cells because nonsense or missense mutations might alter *cld* mRNA levels[80]. Eight candidates were selected for co-expression with LPL in the *cld/cld* cell line derived and immortalized from mice hepatocytes and fibroblasts (MEF)[81]. Only one, *Tmem112,* rescued LPL and HL activity at levels comparable to heterozygous mice and as a consequence it was renamed to *lipase maturation factor 1* (LMF1). Confirming this designation, EL activity in mouse-derived *cld* fibroblasts is rescued by transfection of LMF1[9]. Reverse transcription-PCR in MEFs from cld mice revealed an insertion of a murine retrovirus resulting in a C-terminal truncation in LMF1 of 214 residues[81]. The C-terminal domain of LMF1 contains a conserved domain of unknown function 1222 (DUF1222) but co-localization of LMF1 with the ER-membrane bound calnexin shows that LMF1 resides in the ER. This localization is consistent with a role in protein folding in the ER in agreement with the Endo H data from *cld* mice and the site of LPL maturation.

The topology for mouse and human LMF1 was elucidated using transmembrane prediction methods in combination with biochemical methods[82]. There are five transmembrane domains with the N-terminus is exposed to the cytosol and the C-

terminus facing the ER lumen (**Fig. 1.3**). Consequently, C-terminal truncation variants of LMF1 were generated to study the role of the DUF1222 domain in LPL maturation as well as the interactions of LPL with the ER facing portions of LMF1 (loop A and C see **Fig. 1.3**). C-terminal truncations that entirely or partially remove the DUF1222 domain of LMF1 demonstrate these truncations still localize to the ER-lumen. However, neither construct restores LPL activity in the *cld/cld* cell line. Affinity purification of LPL or PL in complex with wild type (WT) or LMF1 variants shows that both lipases bind to loop C but not loop A. The studies with the C-terminal truncations of LMF1 confirmed the role of the DUF1222 domain in processing of LPL in the ER. Additionally, we learned that loop C does not confer LPL activity when it is in combination with loop A but it is necessary to bind LPL. It is likely that the loop C-LPL interaction is necessary for the folding role of the C-terminus of LMF1 on LPL. Lastly, affinity purification of EL and LMF1 complexes from HEK293 cells demonstrate that EL also physically interacts with LMF1[9] although it remains unknown if EL binds to loop C. In contrast to dimeric lipases, the activity of the monomeric PL is not reduced in *cld* cells, and PL does not bind to LMF1[9,83]. Thus it has been suggested that LMF1 is important for the homodimerization of dimeric lipases.

LMF1 mutations in humans are not lethal as they are for *cld* mice that die 2-3 days after ingestion of dietary milk. Humans homozygous for LMF1 mutations can survive to adulthood without detection of severe hypertriglyceridemia as was the case of the first reported LMF1 mutation, Y439X[81]. The subject's hypertriglyceridemia was not detected until 18 years of age with attacks of pancreatitis starting at age 27 despite a strict diet of 20 grams of total fat daily. The second nonsense mutation identified

localizes to residue W464. Similar to mice, the homozygous defect confers lipid accumulation whereas the subject's son is heterozygous for the mutation and has normal TG levels. Functional analysis of both nonsense mutations in *cld* MEFs showed that the W464X mutation restores more LPL activity than the Y439X mutant, resulting in slightly better LPL secretion but not enough to prevent severe hypertriglyceridemia[84].

Even though three dimeric lipases are dependent on LMF1 for activity, we will focus our studies on LPL maturation. LPL is the only dimeric lipase deficiency that is lethal in homozygous mice[85] plus it is the rate-limiting enzyme for the hydrolysis of TG within the capillary lumen and several LPL mutations have been implicated in severe hypertriglyceridemia, atherosclerosis, and coronary artery disease in humans.

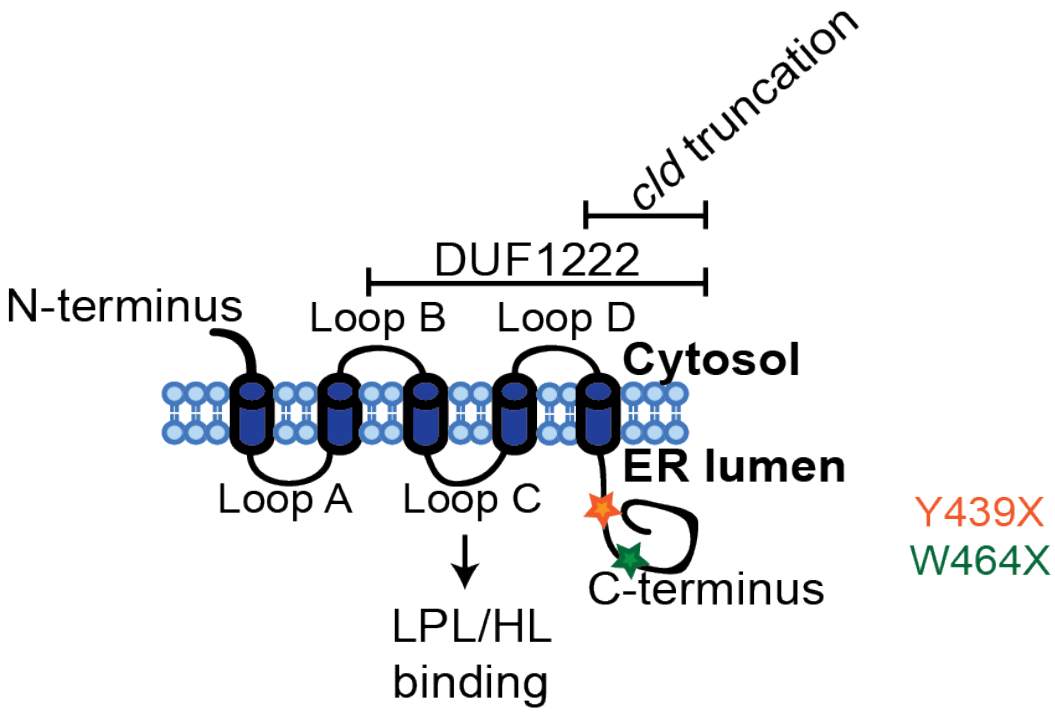

Figure 1.3 Schematic of LMF1 topology and summary of experimentally supported facts.
LMF1 contains five transmembrane domains with loop A, loop C, and the C-terminus facing the ER lumen to promote dimeric lipase maturation. Human LMF1 is 567 amino acids (aa) long whereas mouse LMF1 is 574 aa long. The approximate size of each domain is: N-terminal 49 aa, loop A 56 aa, Loop C 71 aa, loop D 46 aa, and C-terminal 188. The Y439X truncation removes 127 residues from human LMF1 while W464X removes only 103.

Despite the similarity of the phenotype from the *cld* mice with LPL and LMF1 deficiency in humans, development of null LMF1 mice was needed to truly understand LMF1 deficiency in mice. The naturally occurring *cld* mutation in mice localizes to a variant of chromosome 17 known as the *t* haplotype, a region that contains mutations affecting several genes. As a result, the phenotype of the *cld* mice might include effects from other genes. Furthermore, the *cld* truncation variant of LMF1 expresses in HEK293 cells and localizes in the ER. Thus, the allele could be hypomorphic, which would allow some expression of ~60% of LMF1. In agreement with *cld* mice, LMF1 null mice develop severe hypertriglyceridemia within 24 hrs after birth[86]. These mice also have a reduction in LPL and HL activities in the plasma. Their plasma lipoprotein profile demonstrates the high TG levels are due to accumulation of chylomicrons and VLDL; TG accumulation as well the impairment of lipase activity is not observed in heterozygous or WT littermates. Thus LMF1 null mice recapitulate the phenotype observed in *cld* mice confirming that the phenotype previously observed is indeed consequence of only LMF1 deficiency. Lastly, LMF1 is ubiquitously expressed but the null LMF1 mice demonstrate that LMF1 not needed for embryonic viability[81,86].

Mutations associated with severe hypertriglyceridemia

Severe hypertriglyceridemia is a condition characterized by plasma triglyceride levels greater than 1,000 mg/dL (>11.3 mmol/liter)[87]. LPL deficiency results in accumulation of CM and VLDL that leads to severe hypertriglyceridemia. LPL deficiency is an autosomal recessive disorder caused by loss of function mutations in the LPL gene. The frequency of LPL deficiency is 1 in half a million and it typically presents at childhood with abdominal pain, eruptive xanthomas, lipemia retinalis, and recurrent pancreatitis. Nearly 100 LPL mutations have been identified in humans. These mutations can abolish LPL's catalytic function or prevent interaction with ApoCII, ApoAV or GPIHBP1 and hence result in severe hypertriglyceridemia[88-90]. Mutations in genes that interact with LPL also result in severe hypertriglyceridemia. These include ApoCII, ApoAV, GPIHBP1, and LMF1[81,89].

In contrast to the great majority of LPL mutations found to date, population-based studies of LPL variants have revealed a cardioprotective effect for the nonsense mutant S447X. This mutation is found in 20% of the population where it is associated with reduced plasma TG and increased HDL cholesterol[91,92]. As discussed in the next section, this mutant is used as treatment for LPL deficiency.

Current treatments for absence of LPL in the capillary lumen

The usual treatment for people with LPL deficiency is a restricted low fat diet and the utilization of lipid lowering drugs like statins and fibrates. Statins are the main treatment of choice for reduction of LDL in individuals at high risk for atherosclerotic cardiovascular disease[93]. However, a recent study demonstrates that statin treatment is not sufficient to prevent coronary artery disease for individuals with TG levels >150

mg/dl[94]. Fibrates are ineffective for LPL deficiency treatment because they promote LPL expression and repression of ApoC-III through activation of the peroxisome proliferator-activated receptors (PPAR-α)[95]. Additionally, a low fat diet does not eliminate disease progression and pancreatitis episodes. Gene therapy with intramuscular injections of the gain of function LPL mutation S447X has been shown to reduces plasma TG levels in clinical trials[96]. However, TG levels returned to base line after 18-31 months due to an immune response to the AAV1-capsid. A second clinical trial included immunosupressants. Twenty-six weeks post treatment, LPL protein levels were detected in 4 out of 7 samples while LPL activity was detected only in 3[97]. Additionally, after 3-12 weeks of treatment, 50% of the subjects had a ≥40 reduction in plasma TG levels while two subjects had no improvement. More importantly, TG levels return to baseline 16-26 weeks post-treatment. Even though gene therapy with the LPL variant S447X was approved by the European Commission in 2012, the cost for therapy is over 1 million dollars which is not cost effective considering the fleeting effects of the treatment[98]. A more effective treatment is needed for patients with LPL deficiency.

Elevated TG levels and cardiovascular disease

Additionally, elevated TG levels are associated with risk of cardiovascular disease[99]. Data from the American Heart Association shows that one third of adults in the US have borderline high lipid levels, and a further one third have high lipid levels or hypertriglyceridemia[100]. Thus understanding how LMF1 promotes LPL maturation may aid future drug development to treat hypertriglyceridemia. The intracellular pool of inactive and aggregated monomers of LPL destined for ER degradation could be rescued by pharmacological chaperones[66]. Pharmacological chaperones are

compounds that rescue proteins from degradation in the ER by serving as a folding template, restoring activity and trafficking pathways[101,102]. Treatment with pharmacological chaperones for LPL could prevent risk of cardiovascular disease due to high lipid levels.

Summary

Although LMF1 is necessary for maturation of all three dimeric lipases, several questions remain regarding the role of LMF1 in LPL maturation. How is LMF1 retained in the ER lumen? We know that only loop C and the C-terminus domain of LMF1 are known to bind or be necessary for LPL activity respectively. Would a truncation leaving these domains unperturbed be sufficient for LPL processing in the ER resulting in active and secreted lipase? Additionally, it is clear that LMF1 plays a role in the maturation of dimeric lipases. However, the mechanism by which it assists in this process is unclear. What is the role of LMF1 in tissues that do not express dimeric lipases and what are the substrates of LMF1 in those tissues? The remainder of this thesis addresses these questions. Chapter 2 works on the gaps left by the C-terminal truncations of LMF1. Instead we generated N-terminus truncations of LMF1 to determine the minimal domains of LMF1 necessary for secretion of LPL. Lastly, Chapter 3 describes our identification of interacting partners of LMF1 that assist in maturation of LPL and that can shed light on the role of LMF1 in LPL maturation.

CHAPTER 2: PURIFICATION, CELLULAR LEVELS, AND FUNCTIONAL DOMAINS OF LIPASE MATURATION FACTOR 1[1]

Introduction

Lipoprotein lipase (LPL) plays a critical and complex role in lipid metabolism. LPL hydrolyzes triglycerides (TGs) from two classes of circulating lipoproteins, VLDLs and chylomicrons, in order to distribute free fatty acids to peripheral tissues. Biochemical deficiency of LPL activity is one well-established cause of hypertriglyceridemia, which is associated with increased risk of atherosclerosis, acute pancreatitis, and presence of metabolic syndrome[103]. Mutations in both LPL and its interacting partners can result in biochemical deficiency of LPL activity. Here we investigate how one of these interacting partners known as LMF1 promotes LPL activity.

Deleterious mutations in the gene for *LMF1* result in severe hypertriglyceridemia[81,104]. *LMF1*'s precise genetic location was only recently discovered[81], but its role in promoting LPL activity is well established. Mice with a recessive mutation on chromosome 17 were severely deficient for the activity of LPL and the very closely related hepatic lipase (HL)[77]. This mutation was termed *cld*, for combined lipase deficiency[77]. Mice with homozygous disruptions in the *LPL* gene had phenotypes that were nearly indistinguishable from *cld/cld* mice (death within 48 hours of birth with extreme elevations of serum triglycerides[85]. However, the *cld* mutation

[1]The work referenced in this chapter has been published in: Babilonia-Rosa MA and Neher SB. (2014) Purification, cellular levels, and functional domains of lipase maturation factor 1. BiochemBiophys Res Commun. 450,423-8.

clearly did not affect the LPL and HL structural genes, as these genes mapped to different chromosomes[105]. Furthermore, the amount of LPL protein present in tissues was not reduced, but its activity was[106]. LPL activity was reduced because the majority of the LPL was retained in the ER as inactive aggregates in *cld/cld* cells[83]. Recently, the *cld* mutation was mapped to a gene coding for an ER-resident, transmembrane protein, and renamed *LMF1*, for lipase maturation factor 1[81]. Subsequently, LMF1 was found to be important for the activity of a third dimeric lipase, endothelial lipase[9].

Although LMF1 is vital for secretion of active, dimeric lipases, it is not clear how it promotes the exit of dimeric lipases from the ER. It is therefore important to determine which domains of LMF1 contribute to dimeric lipase maturation. Mapping studies of LMF1's domain architecture reveal that it has a total of five transmembrane domains with its N-terminus in the cytosol and its C-terminus in the ER lumen[82]. The loops connecting these transmembrane domains are labeled A-D and are diagramed in Figure 1A. Recent data suggest that loop C and the C-terminus of LMF1 are important for dimeric lipase maturation[82]. The importance of LMF1's C-terminal, ER resident domain was established in studies of the original *cld* mutation and in patients with *LMF1* mutations. Two nonsense mutations in the C-terminal ER domain of LMF1 (Y439X and W464X) resulted in truncated variants that were unable to assist dimeric lipases in the maturation process[81,104]. Additionally, co-immunoprecipitation studies performed on C-terminal LMF1 truncations showed that loop C is important for interaction with dimeric lipases[82]. Before this current study, nothing was known about the role, if any, of the N-terminal portions of LMF1.

Here, we sought to determine which of LMF1's domains are essential for its function and how LMF1 interacts with LPL by measuring the cellular levels of both proteins. To determine if the C-terminal portions of LMF1 were sufficient to promote dimeric lipase maturation, we made N-terminal LMF1 truncation variants. We show that these LMF1 truncations are properly localized and oriented in ER membrane. However, expression of these constructs in *cld/cld* cells show that the entire LMF1 protein is required for maturation of LPL. We generated a high-affinity, polyclonal antibody using purified LMF1. We found that endogenous LMF1 levels are very low, and each LMF1 molecule promotes the maturation of at least 50 molecules of LPL.

Experimental procedures

Expression constructs

Constructs for the expression of CD3δ-YFP and CFP-CD3δ[107] and mCherry-KDEL (mCh-KDEL)[108] have been described. The coding sequence of human LPL was amplified from pCMV-SPORT6-LPL (Open Biosystems) with a C-terminal V5 epitope tag and inserted into the NheI and XbaI sites of pIRES-EGFP (Addgene). For LMF1 variants, the cDNA for human LMF1 was obtained from Open Biosystems (ID 100062174) and inserted into the BamHI/Xho1 sites of pcDNA5/FRT/TO with an 8x C-terminal polyhistidine tag. The forward primer for TM3 (5'-tcccggattgtcctgtggggc-3') and TM5 (5'-tcccggattgtcctgtggggc-3') were selected based on computational models for the topology of human LMF1[82]. Both LMF1 truncations included an N-terminal MHRRRS ER retention signal from human invariant chain isoform Iip33[109] and an 8x C-terminal polyhistidine tag. To generate pFastbacLMF1, the coding sequence for human LMF1

was amplified with an added C-terminal polyhistidine tag and inserted into the Spe1 and Xba1 sites of pFastbac1 (Invitrogen).

Cell lines, transfection, and media collection

COS-7, *cld/cld* and *cld/wt*[110] cell lines were maintained at a split ratio of 1:10 in Dubelcco's modified Eagle's medium, 10% fetal bovine serum, 1% penicillin/streptomycin, and 1% L-glutamine (complete medium). Transfections were performed with 2 mg of DNA and X-treme gene (Roche Applied Science) according to manufacturer's instructions. COS-7 cells were transfected using Fugene 6 (Promega) with 0.3 mg of mCh-KDEL, 1.7 mg of LMF1 constructs, and 1 mg of CD3δ-YFP and CFP-CD3δ. Cells were transfected 24 hours after plating and harvested 24 h post-transfection. For secretion experiments, the media of *cld/cld* or *cld/wt* cells was changed to complete media but with 1% FBS and 15 u/mL of heparin 3 hours prior collection, 600 µL media was used per 9.5 cm^2 well.

Western blot analysis

Cells were lysed 24 hours after transfection using lysis buffer (150 mM NaCl, 1% Triton X-100, 50 mM Tris pH 8). The pellets were re-suspended with 3X SDS loading dye diluted with 8M urea. Media, lysate, and pellet samples were separated using 12% SDS-PAGE. Proteins were transferred to PVDF (Millipore) and blocked with 5% nonfat milk in TBS-T. For LMF1 Westerns, chicken anti-LMF1 antibody was used at 1:10,000, AP-conjugated anti-chicken (Thermo Scientific) was used at 1:5000, and Westerns were developed using ECF reagent (GE Healthcare). Epitope tags were detected with anti-His and anti-V5 antibodies diluted 1:5000 (both mouse, Thermo Scientific). Mouse anti-GAPDH (Millipore) was used at 1:20,000, and HRP-conjugated anti-mouse (Southern

Biotech) was used at 1:20,000. Rabbit anti-progesterone receptor (PR, Santa Cruz) was used at a 1:100 dilution. HRP-conjugated secondary antibodies were used at 1:5000. Westerns were developed using ADVANSTA WesternBright reagent (Bioexpress).

Indirect Immunofluorescence

COS-7 cells were plated to 70% confluency on glass coverslips. Twenty-four hours post-transfection, the cells were fixed with 4% paraformaldehyde in PBS for 15 min. Cells were washed three times with PBS then incubated for 10 min with 0.1% triton X-100 and 100 mM glycine. Coverslips were washed three times with PBS, then blocked with 2% BSA for 30 minutes, and incubate with anti-his antibody (1:200 in 2% BSA) for 1 hour at room temperature. Secondary antibody (Alexa Fluor 488-conjugated anti-mouse, Molecular Probe) was diluted 1:800 in 2% BSA and incubated for 1 hour at room temperature in darkness. DAPI (Sigma-Aldrich) was used at 0.8 mg/mL for 10 minutes. After further washing in PBS, coverslips with cells were mounted facedown onto glass slides (Fisher) using ProLong Gold Antifade (Molecular Probes). Cells were examined at room temperature under a Zeiss LSM 710 confocal microscope with a 63X oil/1.4 Plan Apo.

Protease protection assay (PPA)

The PPA was performed as described[111] with the following modifications. COS-7 cells were permeabilized with 120 μM digitonin (Sigma Aldrich) for 1 min followed by 20 μM trypsin (Sigma Aldrich) incubation for 1 or 2 min. Complete medium was added to stop trypsin cleavage. The cells were spun at 9000 RPM for 5 minutes, washed with PBS, and lysed with lysis buffer for 30 minutes. Samples were analyzed by Western blotting as above. LMF1 and GFP were detected with anti-his and anti-GFP (rabbit,

Abcam) antibodies, respectively, at 1:5000. HRP-conjugated secondary antibodies were used at 1:20,000.

Protein purification

LPL-V5 was purified essentially as previously described[61]. LMF1 was expressed in SF9 cells. Bacmids generated as per manufacture's instructions (Invitrogen) were transfected into SF9 cells using Xtreme gene (Roche). Baculovirus was amplified for three passages and used to infect SF9 cells. Infected cells were harvested after 72 hours, resuspended in Buffer 1 (20 mM Tris pH 7.5, 100 mM NaCl, and 5 mM β-mercaptoethanol) with added complete protease inhibitor (Roche). Cells were lysed with 2 passes through an EmulsiFlex (Avestin). Lysate was spun at 100,000 xg for 1 hour. The pellet was resuspended in Buffer 1 and dounced until in solution. Fos-Choline 12 was added to 20 mM, the solution was rocked overnight at 4°C and then spun at 100,000 xg for 1 hour. The supernatant was load onto Ni-NTA (Qiagen), washed with Buffer 1 plus 3 mM Fos-Choline 12, and eluted the same buffer plus 400 mM imidazole. Eluate fractions containing protein were loaded onto a MonoS column in Buffer 1 plus 3 mM Fos-Choline 12 and eluted over 15 column volumes to Buffer 2 (20 mM Tris pH 7.5, 1M NaCl, 1 mM DTT, 3 mM Fos-Choline 12). Select fractions were further separated on S200 in Buffer 3 (20 mM Tris pH 7.5, 100 mM NaCl, 1 mM DTT, 3 mM Fos-Choline 12, 10% glycerol). Fractions were flash frozen on liquid nitrogen.

Antibody production

Antibodies against purified LMF1 were raised in chickens according to standard protocol (Covance) and purified as described[112].

Genomic PCR

DNA was isolated from *cld* cell lines with DNeasy kit (Quiagen) according to manufactures directions. The primer sequences used to distinguish between WT LMF1 and *cld* LMF1 have been described[81].

Results

The C-terminus of LMF1 is not sufficient for dimeric lipase maturation

The C-terminal, ER resident domain of LMF1 is necessary for efficient exit of LPL from the ER[81,104]. However, the importance of the N-terminal portions of LMF1 in LPL maturation is not known. To identify the minimal LMF1 construct that can support LPL maturation, we made two N-terminal truncations of LMF1 (**Fig. 2.1A**). To ensure that these truncation variants were properly targeted to and retained in the ER, we added a short, N-terminal motif from the human invariant chain isoform Iip33 previously shown to target an unrelated membrane protein to the ER[109]. This Iip33 segment replaced N-terminal portions of LMF1 in two truncation constructs named TM3 and TM5 (**Figure 2.1A**). TM5 is comprised of only the C-terminal ER domain whereas TM3 has this domain plus loop C, which was previously shown to be important for binding to LPL [82]. These truncations allowed us to test the role of loop C and the C-terminus of LMF1 independently. Full length (FL) LMF1, TM3 and TM5 all have C-terminal His tags for uniform detection, and all were transiently transfected in *cld/cld* cells. As expected, FL, TM3, and TM5 were detected by Western blot at 60, 43, and 27 kDa (**Fig. 2.1B**). TM5

was highly expressed and so 5-fold less protein was loaded to allow detection of the other LMF1 variants. No LMF1 was detected in the soluble fraction, showing that the truncation versions localize to the membrane as expected.

Next, C-terminally V5-tagged LPL was co-expressed with each of the three LMF1 constructs in *cld/cld* cells to determine the minimal domain of LMF1 sufficient for LPL maturation. Heparin was added to the media to induce release of LPL from the cell surface into the media. LPL is expressed in cells with all LMF1 constructs, as it is detected in the lysate and pellet fractions (**Fig. 2.1C**). However, LPL is only secreted when FL LMF1 is present (**Figure 2.1C**, media fraction). Taking into account that only $1/5^{th}$ of the TM5 pellet was loaded, there is more LPL in the pellets of TM3 and TM5 than in the FL LMF1 pellet fraction. This suggests that when FL LMF1 is not present, LPL can't fold properly and is not able to exit the ER, as shown for cells lacking $LMF1^{113}$. Taken together, the release of LPL into the media only with FL LMF1 and the accumulation of LPL in the pellets when co-expressed with the TM3 and TM5 truncations indicate that FL LMF1 is needed for the maturation process of LPL.

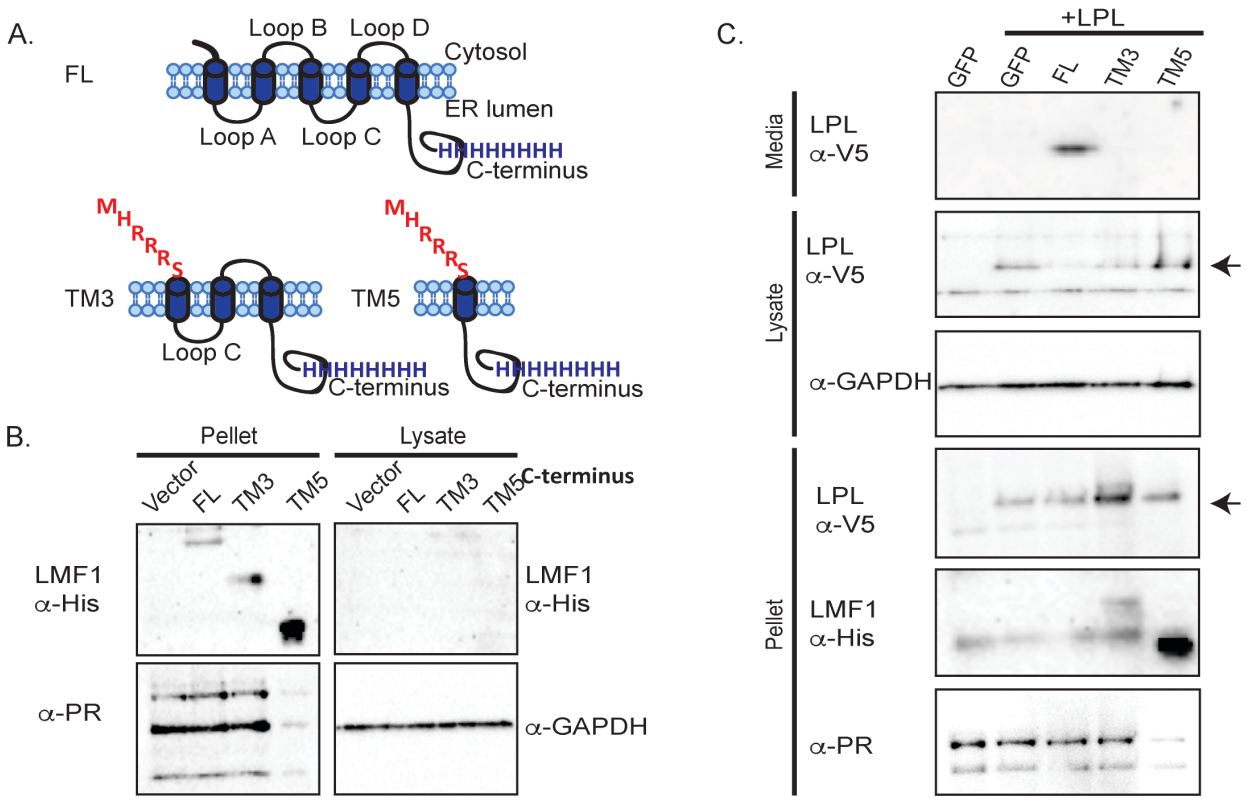

Figure 2.1 The N-terminal domain of LMF1 contributes to LPL maturation. A) A schematic of full length (FL) LMF1's topology as well as both N-terminal truncations. The MHRRRS sequence was added as an ER retention signal. B) Western blots against the C-terminal His tag show that FL, TM3 and TM5 truncations are associated with the pellet fraction. Loading controls include GAPDH for soluble proteins in the lysate fraction and PR for membrane proteins. C) Western blots of the media fraction show that LPL-V5 is secreted in *cld/cld* cells co-expressing the FL, but not the TM3 or TM5, LMF1 constructs. In all panels, 1/5 as much of the TM5 was loaded to allow detection of the other constructs because TM5 was highly expressed.

Localization of LMF1 constructs by fluorescence microscopy

To ensure that the N-terminal ER retention signal from Iip33 properly targeted both LMF1 truncation variants to the ER we tested for co-localization with an ER marker (mCh-KDEL) by immunofluorescence. COS-7 cells were co-transfected with LMF1, TM3, or TM5 and mCh-KDEL. **Figure 2.2** shows that LMF1 co-localizes with mCherry-KDEL. The merge of the two bottom panels of Fig. 2 shows that both LMF1 truncation variants co-localize with mCh-KDEL as well as FL LMF1 does. We can conclude that although TM3 and TM5 are not sufficient to promote LPL maturation, both truncations are present in the ER.

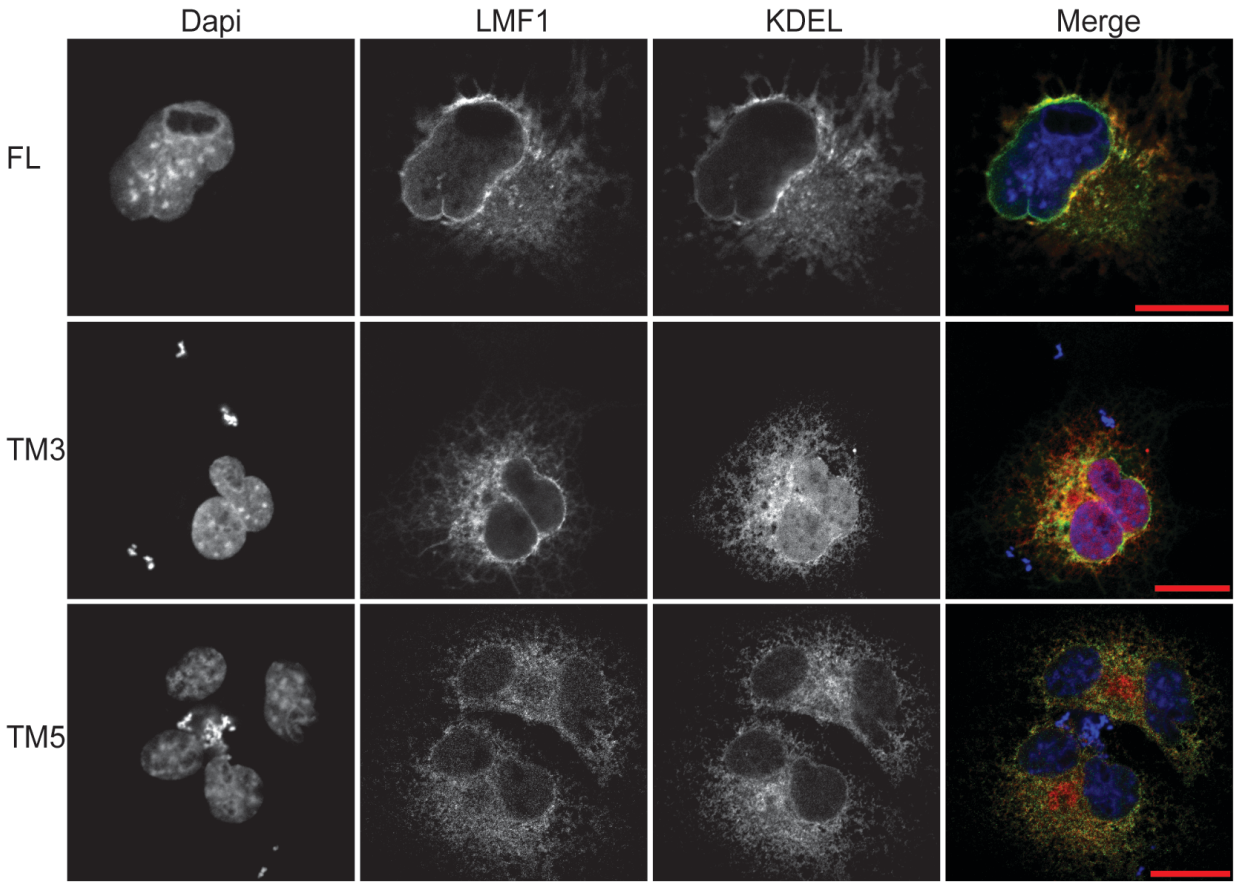

Figure 2.2 LMF1 truncation variants localize to the ER.
Immunocytochemistry of the LMF1 variants (green) was compared to the ER marker mCh-KDEL (red) in COS-7 cells. All LMF1 constructs show perinuclear staining characteristic of the ER as is confirmed by co-localization with mCh-KDEL. Scale bars represent 20 μm.

Membrane topology of LMF1 constructs

Truncation of the N-terminus of LMF1 could result in insertion of the protein into the ER with an incorrect orientation. We therefore performed a protease protection assay (PPA) to determine the orientation of the LMF1 truncations in the ER. In this assay, the plasma membrane is selectively permeablized with digitonin followed by trypsin treatment[111]. Trypsin will cleave membrane domains not protected within the lumen of organelles. COS-7 cells transfected with CD3δ-YFP (CD3δ with a YFP tag exposed to the cytosol) served as a positive control for trypsin cleavage (**Fig. 2.3A**, left panel). CD3δ with a CFP tag protected by the ER lumen (CFP-CD3δ) was a negative control to ensure that the organelles were preserved at the digitonin conditions used. Figure 3A shows complete loss of CD3δ-YFP signal within 2 minutes of trypsin exposure whereas incubation with digitonin alone does not result in YFP degradation. The right panel of **Figure 2.3A** shows no degradation of the 50 kDa CFP-CD3δ band, confirming that the assay conditions leave the ER membrane intact.

We next tested if FL, TM3 and TM5 LMF1 were properly oriented in the ER. If these proteins have the correct topology, their C-terminal His-tags will be trypsin resistant. Unlike CFP-CD3δ, which has ER-protected CFP attached to a single transmembrane domain, we expected that LMF1 will show some cleavage products after trypsin treatment. Human LMF1 has 5 transmembrane domains with 16 cytosolic trypsin cleavage sites (PeptideCutter). Trypsin could cut LMF1 multiple times but only the products attached to the C-terminal His-tag will be detected. Following trypsin addition to cells expressing FL LMF1, we detect bands corresponding to both the full protein (60 kDa) and cleavage products. The cleavage products, ranging from 27 to 20

kDa, are likely due to the 7 trypsin sites in the last cytosolic loop of LMF1 (**Fig. 2.3B**, left panel). After trypsin treatment uncleaved TM3 was present at 43 kDa in addition to lower molecular weight cleavage products (**Fig. 2.3B**, middle panel). For TM5 (**Fig. 2.3B**, right panel); uncleaved TM5 appears at about 27 kDa. The band profile is not altered upon trypsin addition because no exposed cytosolic loops are expected in this construct. Retention of the majority of the signal from the His-tag following trypsin treatment indicates that TM3 and TM5 have their C-termini located in the ER. Thus, the lip33 ER retention signal targets the LMF1 truncation constructs to the ER with the same membrane orientation as WT LMF1.

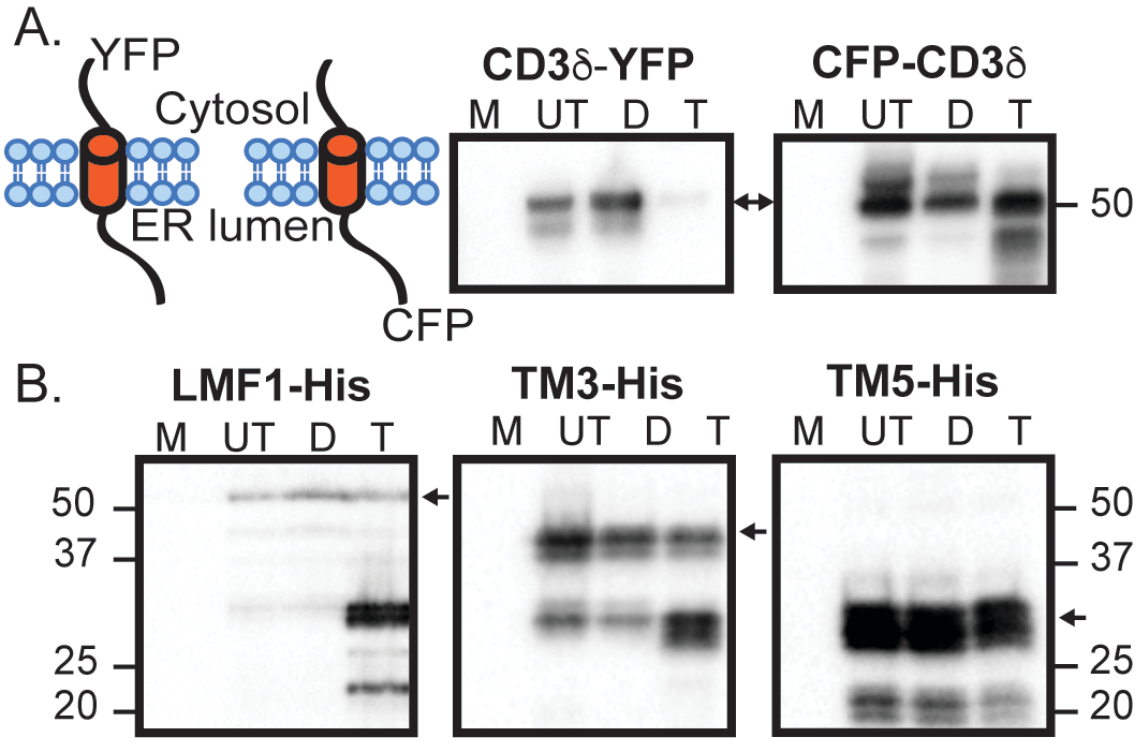

Figure 2.3 Topology of LMF1 truncations.
A) A schematic of the CD3δ constructs used as positive and negative controls for trypsin cleavage, CD3δ-YFP and CFP-CD3δ respectively. The middle and right panels show the western blots for expression and the PPA. Lane 1 was mock (M) transfected, lane 2 shows untreated cells (U), lane 3 has 120 μM digitonin (D) addition for 3 minutes, and lane 4 has 20 μM of trypsin (T) for 2 minutes (after a 1 minute incubation with digitonin). Arrows indicate the FL version of each construct. B) Expression and PPA for WT LMF1 and the two truncation constructs. Lanes are labeled as in A.

Low level LMF1 expression is sufficient for LPL secretion.

The relative expression levels of *LMF1* mRNA have been compared across different tissue types, but little is known about LMF1 protein levels[81]. We generated an antibody against LMF1 to better understand its cellular levels. LMF1 was expressed in SF9 cells and purified to homogeneity as shown by coomassie staining and gel filtration (**Fig. 2.4A**). Purified protein was used to raise antibodies against LMF1 in chickens. This antibody could detect as little as 17.5 fmoles of purified LMF1 (**Fig. 2.4B**). However, Western blots using this antibody failed to detect a specific band for LMF1 in the *cld/wt* vs. *cld/cld* cells (**Fig. 2.4B**). When we transfected a plasmid containing *LMF1* under the control of a CMV promoter into the cells, a band at the expected molecular weigh of LMF1 appeared (**Fig. 2.4B**).

Because we could not detect endogenous LMF1 in *cld/wt* cells, we wanted to ensure that both cell lines had the expected genotype. We confirmed the correct genotype of these cells by analysis of the genomic DNA. Genomic DNA was harvested and tested by PCR for insertion of the murine endogenous retrovirus into intron 7 of *LMF1*, which defines the *cld* mutation (**Fig. 2.4C**)[81]. Bands of the expected size were observed (**Fig. 2.4C**) indicating that LMF1 is present in the *cld/wt* but not the *cld/cld* cells, as expected.

We cannot report the exact number of LMF1 molecules per cell, but can calculate an upper limit. The assays in figure 4B used 1×10^4 cells. Additionally, the membrane fraction of a greater number (1×10^6) of *cld/cld* and *cld/wt* cells was harvested, solubilized, and probed for LMF1 (data not shown). Based on these cell counts and the detection limit of our antibody, we can conclude that there are less than 10,000

molecules of LMF1 per cell, a relatively low expression level. A large-scale proteomics analysis of mammalian cells indicates that approximately 75% of proteins are expressed at higher levels[114,115]. Indeed, whereas LMF2 was identified in this analysis, LMF1 was not[114,115]. We next quantified the amount of LPL-V5 secreted into the media per cell using purified LPL-V5 as a standard (**Fig. 2.4D**). These experiments revealed that, over a 3-hour period, approximately 50,000 molecules of LPL were secreted/cell. Thus, each molecule of LMF1 can promote the maturation of 50 or more molecules of LPL.

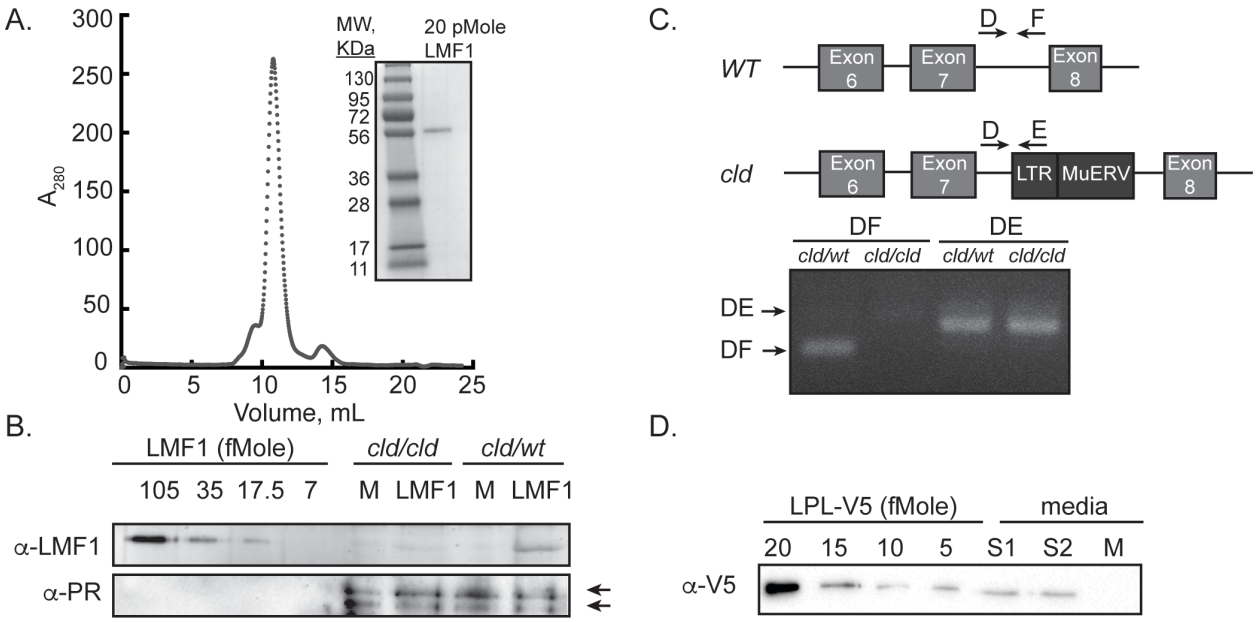

Figure 2.4 LMF1 purification and cellular levels.
A) Gel filtration trace of purified LMF1 shown with a coomassie stained gel. B) Western blot showing that an antibody raised against LMF1 can detect as little as 17.5 fmole of the purified protein. Cells are mock transfected (M) or transfected with a plasmid expressing LMF1. PR is a loading control for the pellet fraction. Arrows indicate both PR isoforms. C) Western blot for quantification of LPL released from *cld/wt* cells. D) LPL is better secreted from *cld/wt* than *cld/cld* cells, as expected. E) Top is a schematic showing oligos (D, E, F) used to test for the insertion of the murine endogenous retrovirus into intron 7 of *LMF1*. PCRs, below, show that *cld/wt* and *cld/cld* cells have the expected genotype.

Discussion

Previous studies on LMF1 have focused on the C-terminus. In patients with defective LMF1, mutations are located in the C-terminus and *in vivo* co-IP's show that loop C of LMF1 binds to LPL[81,82,104]. Based on these findings, we hypothesized that LMF1's C-terminus is not sufficient for the maturation of dimeric lipases but the C-terminus in combination with loop C would promote lipase maturation. To test this hypothesis, we made truncations of LMF1 starting from the N-terminus. Because LPL must be properly folded to enter the secretory pathway[83], we tested LPL secretion into the media in cells expressing only the N-terminally truncated variants of LMF1. These data show that FL LMF1 is required for the maturation process of LPL. Because the ER retention signal of LMF1 is not known, we used the ER retention signal of Iip33 to ensure ER localization of the truncated variants. To demonstrate that the TM3 and TM5 LMF1 truncations did not compromise ER localization and the luminal orientation of the C-terminus, we co-localized LMF1 with an ER marker and performed a protease protection assay. The results of these combined experiments demonstrate that TM3 and TM5 LMF1 have the same localization and topology as FL LMF1. However, they cannot promote the maturation of LPL, indicating that the N-terminus has an important, but unknown function.

We generated a polyclonal antibody to measure LMF1 protein levels. This antibody was very sensitive but could not detect endogenous levels of LMF1. We calculated that there are at most 10,000 molecules of LMF1 per cell, and that each molecule of LMF1 assisted in the maturation of at least 50 molecules of LPL during a 3-hour period. These data give some hints at LMF1 function. Because LMF1 protein is

present at a relatively low level compared to general chaperones like GRP78, calnexin, and calreticulin, which are present at over 1,000,000 molecules per cell, it must perform a specialized function[114,115]. Additionally, LMF1 has a catalytic role because each molecule can efficiently promote the maturation of multiple molecules of LPL.

It is widely accepted that LMF1 is required for maturation of dimeric lipases, but it is not known if LMF1 coordinates the activities of other interacting partners. FL LMF1 is required for lipase maturation, but only loop C and the C-terminus have a known role. This suggests that other domains of LMF1 could interact with binding partners required for lipase maturation. Supporting this idea, we were unable to detect a strong, direct interaction between purified LPL and LMF1 *in vitro* (data not shown). Additionally, real time-PCR analysis shows that LMF1 mRNA is expressed at higher levels in tissues that lack dimeric lipases, such as the pancreas and testis, compared to tissues expressing dimeric lipases[81]. Future studies will be needed to determine if LMF1 requires interacting partners to promote lipase maturation as well as if LMF1 has a role other than lipase maturation in other tissues.

CHAPTER 3: NOVEL BINDING PARTNERS OF LMF1 SUGGEST A ROLE IN OXIDATIVE FOLDING IN THE ER

Introduction

LPL is a secreted, dimeric lipase that hydrolyzes triglycerides present in the lipoproteins VLDL and chylomicrons. Because LPL is rate limiting for clearance of triglycerides from the plasma, LPL deficiency results in severe hypertriglyceridemia. As a secreted protein, LPL transits the ER where its two N-linked glycans and five disulfide bonds are processed. LPL also requires a specialized factor, LMF1, for proper folding and exit from the ER[81]. When LMF1 is absent, LPL forms disulfide-bonded aggregates in the ER, resulting in a phenotype similar to LPL deficiency[83,116]. LMF1 assists in the maturation of not only LPL but also the related, dimeric lipases endothelial lipase (EL) and hepatic lipase (HL)[81]. Pancreatic lipase, a sequence-related, but monomeric lipase, does not require LMF1.

LMF1 is a ER-resident membrane protein that has 5 membrane-spanning domains, resulting in two loops and a large C-terminal domain in the ER lumen[117]. Known deleterious mutations that prevent LPL secretion are located in the C-terminal, ER resident domain[81,84]. *In vivo* pull down experiments showed that loop C interacts with LPL[117]. Finally, our N- and C–terminal truncation experiments show that every ER resident loop of LMF1 is required for LPL maturation[118].

LPL has ten cysteines conserved across species that are known to form five disulfide bonds[1,4]. Three of these disulfide bonds are critical for the activity of LPL

(C216/C239, C264/C275, C278/C283)[73]. Protein folding and quality control in the endoplasmic reticulum (ER) requires not only oxidation of thiols to form disulfide bonds but also reduction of disulfide bonds to facilitate the degradation of misfolded proteins. Members of the disulfide isomerase (PDI) family mediate this thiol-disulfide exchange in eukaryotes[119]. Although glutathione powers the reduction of disulfide bonds[120], eukaryotes have long been hypothesized to utilize another source of reducing equivalents. The bacterial transmembrane electron transporter, DsbD transfers two electrons from thioredoxin to the protein disulfide isomerase DsbC for formation of nonconsecutive disulfide bonds[121]. DsbC must remain in a reduced state to initiate isomerization and DsbD is required to maintain DsbC in a reduced state[122].

In order to understand how LMF1 promotes LPL maturation we took two approaches. First, we developed lipase chimeras with the LMF1-independent PL to determine what region of LPL interacts with LMF1. The chimeras revealed that the C-terminus of LPL binds to LMF1 and this interaction is important for dimeric lipase secretion. Second, we utilized crosslinkers and proteomics to identify binding partners of LMF1. We uncovered a number of ER-resident oxidoreductases as well as thioredoxin (TRX), a cytosolic protein. We further show that TRX, ERp44, and ERdj5 bind to LMF1 in the absence of a crosslinker. In combination these data suggest that LMF1 acts like the bacterial protein DsbD, which shuttles electrons across the periplasmic membrane to DsbC.

Experimental procedures

Expression constructs

Constructs for wild type LMF1 and the C-terminal truncations with an 8X C-terminal polyhistidine tag were previously described[123]. Site directed mutagenesis of LMF1-His was employed to obtain C to A mutations via two single-primer reactions in parallel[124]. The orthogonal pair of suppressor tRNA (*B. stearothermophilus*) and tRNA synthetase (*S. cervisiae*) for photocrosslinking were provided by P. Schultz (The Scripps Research Institute)[125]. AvrII and BsrGI sites were used to remove GFP from the pSWAN-GFP37TAG and insert LMF1 (Open Biosystems) with an 8X C-terminal polyhistidine tag. The amber codon was incorporated in the pSWAN-LMF1 in residue F262 using site directed mutagenesis. Human LPL was excised from pCMV-SPORT6-LPL (Open Biosystems), a C-terminal V5 tag was added, and it was inserted into a pcDNA5/FRT vector (Thermo Fisher Scientific) using HindIII/BcII sites. To clone the lipase chimeras, the pcDNA5/FRT vector was cut with HindIII/Bcl1 and LMF1 was inserted with an N-terminal polylinker containing XmaI, Pme1, and Cla1 sites. The Pme1 and Cla1 sites were used to insert an IRES from the vector pIRES-EGFP (Addgene) into pcDNA5/FRT. Human LPL or PL with a C-terminal V5 tag were inserted using NheI/Xho1 or NheI/Xma1 respectively. PCR-driven overlap extension[126] was used to create a chimera containing the N-terminal of LPL with the C-terminal of PL (LPL/PL) and the reverse construct (PL/LPL). Both chimeras contained a C-terminal V5 tag and were inserted in the modified pcDNA5/FRT. To make the plasmid for expression of TXNIP, the cDNA sequence of human TXNIP was synthesized as a GBlock by IDT. It was digested using A and B enzymes and inserted in pCNDA5/FRT.

Cell lines, transfection, and media collection

HEK 293 Flp-In™ (Thermo Scientific) cells were transfected with LPL-His or LMF1-His using Fugene 6 (Promega) and selected with 200 µg/mL of hygromycin. Regular HEK 293 cells were transiently transfected with Fugene 6 and 1 µg of DNA for LMF1-His and the respective lipase construct for the DSP crosslinking experiment in Figure 3.1C. Transfection of *cld/cld* cells on six well plates was performed with 2 µg of DNA and X-treme Gene HP[127] according to manufacturer's instructions. All cell lines were maintained in Dubelcco's modified Eagle medium with 10% fetal bovine serum, 1% penicillin/streptomycin, and 1% L-glutamine (complete media).

siRNA Knockdowns

siRNA transfections were performed with 20 nM of RNA oligonucleotide and 7 µL of Lipofectamine RNAiMax (Life Technologies) per six-well plate and samples were collected 48 hours post-transfection. Validated Silencer Select siRNAs were obtained from Life Technologies: negative control No. 1 (4390843), ERp44 (s22965), PDI (s439), ERp72 (s18446), UGGT1 (132932), UGGT2 (112074), and ERdj5 (132773). Knockdown was quantitated using a ChemiDoc MP Imaging System from Biorad and quantitated using Image Lab Software. The percent of remaining gene expression was calculated with the following formula: ((Candidate/GAPDH)/(NC/GAPDH))*100. To obtain the percent knockdown = 100 - percent remaining expression.

Crosslinking and pull down assays

For pull down assays of LMF1-His from HEK Flp-In stable cell lines, two T-75 flasks per condition were seeded with 7.5 X 10^6 cells. LMF1-His expression was induced with 2 µg/mL tetracycline the next morning. The next day, cells were trypsinized, washed with 1X PBS, crosslinked with 2 mM DSP (ProteoChem) with agitation for 30 minutes at room temperature, and quenched with 150 mM Tris pH 8. The cells were lysed with by douncing in buffer 1 (250 mM NaCL, 10 mM Tris pH 8, and 1 mM PMSF). Following centrifugation for 20 minutes at 13,000 RPM, the pellets were re-suspended by douncing with 1.4 mL of buffer 1. Lysates were incubated overnight with agitation and the addition of 20 mM fos-choline 12 (Anatrace). After centrifugation as above, 5% glycerol and 40 mM imidazole were added to the supernatant as well as Ni-NTA agarose beads (Qiagen). Binding was allowed for an hour at 4^0C with agitation. The beads were washed 3X with 4 mL of buffer 2 (1M NaCl, 10 mM Tris pH 8, 3 mM fos-choline 12, 5% glycerol, 40 mM imidazole, and 1 mM PMSF) in 11 mL poly-prep chromatography columns (Bio-Rad). LMF1 complexes were eluted with buffer 3 (250 mM NaCL, 10 mM Tris pH 8, 3 mM fos-choline 12, 400 mM imidazole, and 1 mM PMSF). Eluate fractions were loaded on 8% SDS-PAGE, transferred to PVDF (Bio-Rad) for 75 minutes at 100V, and blocked with 5% nonfat milk or BSA.

IP's of LPL-His from HEK Flp-In stable cell lines were carried out similarly. Purification LMF1-His with lipases were carried out similarly but at a smaller scale. Cells were seeded at 6.5 X 10^5 cells per well of 6 well plates (Denville); 3 wells were combined per condition and Fugene 6 or X-treme Gene HP were used, respectively.

For photocrosslinking with pBpa, HEK 293 Flp-In™ stably expressing LPL-V5 were plated in six-well plates at 10.5 X 10^5 cells per well; four wells were utilized per sample. The next day, 1 µg of pBpa plasmid or LMF1-amber construct were transfected with Fugene 6. After 24 hours, the media was replaced with media containing 2 µg/mL of tetracycline, 0.5 mM pBpa (Chem-Impex International), and 0.3% of DMSO. Control wells lacked pBpa but contained 0.3% of DMSO. Cells were grown with pBPA for 24 hours. The media was changed to 1X PBS and the cells were kept on ice and crosslinked with a UV lamp at a wavelength of 365 nm for 30 minutes at 2.5 cm from the lamp. LMF1 was purified from cells as described above.

Lipase secretion

HEK 293 Flp-In stables expressing lipase constructs were induced with 2 ug/mL of tetracycline 24 hrs before media collection. Three hours before media collection, lipase secretion was promoted by addition of 600 µL of DMEM with 1% FBS and 15 u/mL of heparin per 9.5 cm^2 well. For *cld/cld* MEFs, lipase secretion was promoted 24 hrs post-transfection. Samples from lipase secretion experiments were separated using 12% SDS-PAGE.

Antibodies

The epitope tag of LMF1 was detected with an anti-His antibody (1:5,000 AbD Serotec). PDI, ERp72, and ERp44 antibodies were obtained from Cell Signaling, used at 1:1,000 in 5% BSA, and with HRP-conjugated anti-rabbit (Southern Biotech) at 1:5,000. UGGT1, UGGT2, ERdj5, TRX and TXNIP antibodies were obtained Abcam; used at 1:500, 1:1,000, 1:500, 1:1,000, and 1:600 respectively in 5% BSA with HRP-

conjugated anti-mouse or rabbit antibodies from Southern Biotech. Mouse anti-V5 antibody from Bio-Rad was diluted 1:5,000.

Mass Spectrometry

Gel slices containing purified LMF1 with pBPA or DSP-crosslinked binding partners were delivered to the Duke Proteomics facility for analysis by mass spectrometry. Coomassie stained SDS-PAGE bands were subjected to standardized in-gel trypsin digestion (http://www.genome.duke.edu/cores/proteomics/sample-preparation/documents/In-gelDigestionProtocolrevised.pdf). Extracted peptides were lyophilized to dryness and resuspended in 12 uL of 0.2% formic acid/2% acetonitrile. Each sample was subjected to chromatographic separation on a Waters NanoAquity UPLC equipped with a 1.7 µm BEH130 C_{18} 75 µm I.D. X 250 mm reversed-phase column. The mobile phase consisted of (A) 0.1% formic acid in water and (B) 0.1% formic acid in acetonitrile. Following a 3 µL injection, peptides were trapped for 3 min on a 5 µm Symmetry C_{18} 180 µm I.D. X 20 mm column at 5 µl/min in 99.9% A. The analytical column was then switched in-line and a linear elution gradient of 5% B to 40% B was performed over 30 min at 400 nL/min. The analytical column was connected to a fused silica PicoTip emitter (New Objective, Cambridge, MA) with a 10 µm tip orifice and coupled to a QExactive Plus mass spectrometer (Thermo) through an electrospray interface operating in a data-dependent mode of acquisition. The instrument was set to acquire a precursor MS scan from *m/z* 375-1675 with MS/MS spectra acquired for the ten most abundant precursor ions. For all experiments, HCD energy settings were 27v and a 120 s dynamic exclusion was employed for previously fragmented precursor ions.

Raw LC-MS/MS data files were processed in Proteome Discoverer (Thermo Scientific) and then submitted to independent Mascot searches (Matrix Science) against an SwissProt database (*Human* taxonomy) containing both forward and reverse entries of each protein (20,322 forward entries). Search tolerances were 5 ppm for precursor ions and 0.02 Da for product ions using trypsin specificity with up to two missed cleavages. Carbamidomethylation (+57.0214 Da on C) was set as a fixed modification, whereas oxidation (+15.9949 Da on M) and deamidation (+0.98 Da on NQ) were considered dynamic mass modifications. All searched spectra were imported into Scaffold (v4.3, Proteome Software) and scoring thresholds were set to achieve a peptide false discovery rate of 1% using the PeptideProphet algorithm.

NEM Modification

HEK293 cells stably expressing LMF1 variants were seeded in a T75 flask at 5 $x10^6$ cells. LMF1 expression was induced overnight with 2 µg/mL tetracycline. Cells were harvested, washed with PBS and precipitated with 10% TCA. The DTT treated control cells were first treated with 10 mM DTT for 10 minutes. Samples were spun for 10 minutes at 4^0C in a microcentrifuge at 14,000xg, washed with ice cold acetone and resuspended with a mechanical douncer in 2% SDS, 50 mM Tris pH 7.4, 80 mM NEM. The DTT control sample was not treated with NEM. Samples were incubated at 37^0C for 30 minutes, then denatured at 80^0C for 10 minutes. Samples were diluted 10x in Triton Buffer (2% triton, 50 mM Tris pH 8, 150 mM NaCl), cleared by centrifugation, and incubated with 200 µLs Ni-NTA resin. Samples were washed and purified as per the crosslinking assays, except that Triton buffer with 10 mM Imidizole was used for washing and Triton Buffer with 400 mM Imidizole was used for elution.

BSO, DTT, and tunicamycin sensitivity

To assess cell sensitivity to buthionine sulphoximine (BSO), DTT and tunicamycin, first $1x10^5$ cld/cld or cld/wt were plated in a 6-well plate. The next day either a buffer control, 10 mM L-BSO, 2.5 µg/mL tunicamycin or 5 mM DTT was added. After 24 (tunicamycin or BSO) or 12 (DTT) hours of treatment, cells were removed from the plate with trypsin, stained with trypan blue and live cells were manually counted using a hemocytometer.

Results

LMF1 Binds to the C-terminus of LPL

To determine the LMF1 binding site in LPL we generated two LPL-PL chimeras. These chimeras are diagramed in **Figure 3.1A**. The PL-LPL chimeras consist of the N-terminal domain of PL fused to the C-terminal domain of PL, whereas the LPL-PL chimera is comprised of the N-terminal domain of LPL fused to the C-terminal domain of LPL. Both chimeras, as well as the WT LPL and PL controls, have C-terminal V5 epitope tags for uniform detection. As shown in **Figure 3.1B**, all of the lipase constructs are stably integrated into HEK293 cells under the control of a tetracycline inducible promoter. All of the proteins express, as shown in the lysate panel. However, only PL, LPL, and PL/LPL are secreted. Each variant was co-expressed with His tagged LMF1, crosslinked with the amine reactive crosslinker dithiobis-succinimidyl propionate (DSP), and affinity purified via LMF1's His tag to detect interacting lipase constructs. Western blots showed that PL/LPL but not LPL/PL binds LMF1 (**Fig. 3.1C**). Thus, LMF1 recognizes an element in the C-terminal β-sandwich domain of LPL.

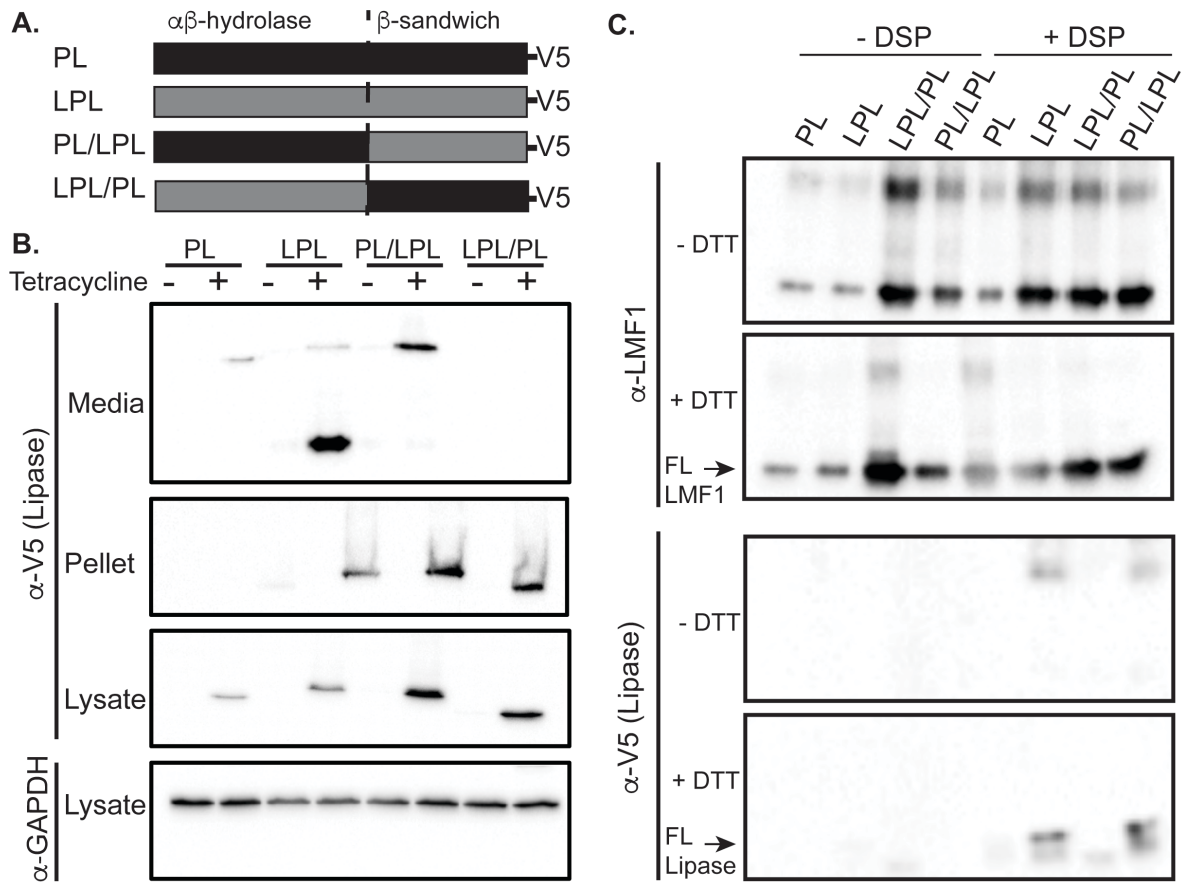

Figure 3.1 LMF1 binds to LPL through its C-terminus.
A) Schematic of lipase constructs. Human LPL has 475 residues while PL has 465. The PL/LPL chimera contains residues 1-341 of the N-terminus of PL and 329-475 of the N-terminus of LPL. Respectively, the LPL/PL chimera contains residues 1-328 of LPL and 342-465 of PL. B) PL/LPL but not LPL/PL is secreted from cells. Tetracycline was added to induce lipase expression in HEK 293 FRT cells with stably integrated lipase constructs. Lipase secretion was induced with heparin. Lipase variants present in the media, lysate and pellet fraction were detected via their C-terminal V5 tags. C) PL/LPL but not LPL/PL is crosslinked to LMF1. LMF1-His was transiently transfected in HEK 293 FRT cells stably expressing a lipase constructs. The crosslinker DSP was added, and LMF1 and associated proteins were purified via LMF1's his tag. Panel 3 shows that only LPL and PL/LPL were detected in a complex with LMF1. The data for Figure 3.1C was provided by Lindsey J. Broadwell.

Identification of novel LMF1 binding Partners

To better understand LMF1's function we next set out to determine which proteins it interacts with in the cell. We used two crosslinking reagents to covalently link LMF1 and its partners during extraction from the membrane. DSP is a homobifunctional, amine reactive crosslinker with a cleavable disulfide bond in its spacer arm. We also used a method for site-specific incorporation of an artificial amino acid into LMF1[128]. In this system, an orthogonal tRNA and aminoacyl-tRNA synthetase pair incorporates an unnatural amino acid into LMF1 at a nonsense codon in a position of our selection. We used the artificial amino acid *p*-benzoylphenylalanine (pBpa), which crosslinks to nearby proteins when UV light is applied to the cells[129].

For DSP crosslinking, HEK293 cells stably expressing LMF1-His under the control of a tetracycline-inducible promoter were treated with crosslinker, and LMF1 was purified as we have previously described[118]. In **Figure 3.2A** a Western blot shows the increase in intensity of a 150 kDa band (asterisk) when LMF1 was induced with tetracycline and crosslinked with DSP. After the crosslinks were released, new bands representing LMF1 binding partners appeared in a gel stained for total protein (**Fig. 3.2B**, asterisks). These bands were identified by LC-MS/MS at the Duke Proteomics Facility. For pBpa crosslinking, we used HEK293 cells transiently transfected with a plasmid bearing the orthogonal tRNA and aminoacyl-tRNA synthetase and a plasmid containing LMF1 with an amber codon and a C-terminal His-tag[130]. We purified LMF1 and bound proteins, performed Western blots and identified robust interactions as shown by the multiple, higher molecular weight bands reacting with anti-His antibody (**Fig. 3.2C,** pBPA panel). Higher molecular weight bands can also be seen in the gel

stained for total proteins (**Fig. 3.2D**, asterisks). We excised these bands and sent them for protein identification by LC-MS/MS. The corresponding gel region of a sample without added pBpa served as a negative control.

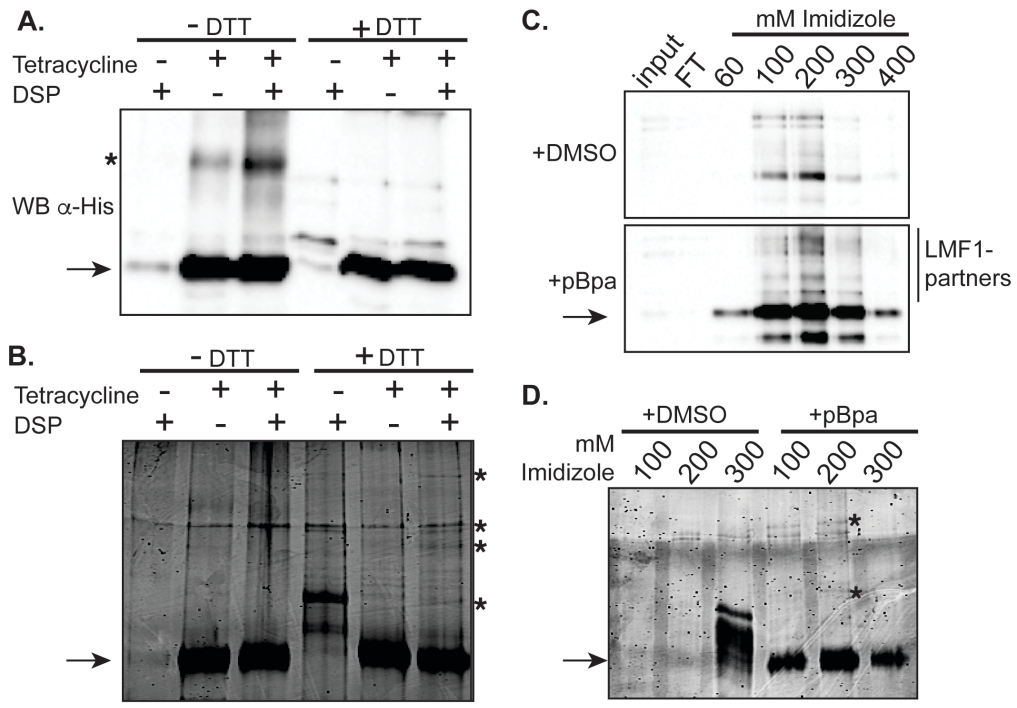

Figure 3.2 Identification of new LMF1-interacting partners.
A) Western blot of LMF1-partners after DSP crosslinking and affinity tag purification using LMF1's C-terminal His tag. Tetracycline induces LMF1 expression. Loading dye with 50mM DTT was used to break the disulfide bonds between LMF1 and its interacting partners. LMF1 complexes are labeled with asterisks and an arrow points to FL LMF1. B) SYPRO orange protein stain of DSP crosslinked samples. Samples without tetracycline but with DSP and DTT, and with tetracycline, DSP and DTT were sent for LC MS/MS. C) and D) Western blot and SYPRO orange stained gel of LMF1-partners after pBpa photo-crosslinking and affinity tag purification. The DMSO panel does not include pBpA and serves as a negative control. pBpa was added to the second sample so LMF1 complexes can be detected. Fractions were eluted with increasing concentrations of imidazole.

Over 300 proteins in total were identified in the two samples. We selected candidates identified with 95% or greater confidence with more peptides identified in the LMF1-containing sample than a control sample. Additionally, for pBpa the predicted molecular weight of the LMF1-candidate protein complex had to fall within or exceed the molecular weight range corresponding to LMF1 plus the molecular weight of the candidate. For both crosslinkers, we focused on proteins annotated as residing in the ER. **Tables 3.1** and **3.2** list protein candidates that meet these criteria for DSP and pBpa respectively. Of note, we found SEL1L, a known LMF1-interacting protein, through our DSP crosslinking[131]. Additionally, in agreement with a proteomics study that isolated interacting partners of hepatic lipase, we found proteins associated to the calnexin/calreticulin system, Bip, protein disulfide isomerase A3 (ERp57), and proteins involved in ERAD which are highlighted in bold in **Tables 3.1** and **3.2**[132].

Table 3.1 Mass spectrometry candidates from DSP crosslinking.

Protein	Function	Unique Peptides	% Coverage	tet/ notet
78 kDa glucose-regulated protein (GRp78 or Bip)	Protein folding and ERAD	7	13	23/8
Calnexin	Assist protein assambley or ER-retention of missfolded proteins.	6	12	22/9
Neural aplha-glucosidase AB (GANAB)	Cleavage of the 2 innermost glucose residues of oligosaccharide from immature glycoproteins	11	18	19/11
UDP glucose:glycoprotein glucosyltransferase 1 (UGGT1)	Reglucosidates glycoproteins with minor folding defects.	6	6	17/6
Tanslocation protein SEC63 homolog	Translocation of proteins to the ER.	8	16	15/8
Lipase maturation factor 1 (LMF1)	Nessesary for the maturation of dimeric lipases in the ER.	3	6	14/4
Transitional endoplasmic reticulum ATPase (TER ATPase)	Involved in the formation of the transitional ER, fragmentation of Golgi stacks and ERAD.	9	13	13/9
Sarcoplasmic/endoplasmic reticulum calcium ATPase 2 (ATP2A2)	Translocation of calcium from the cytosol to the sarcoplasmic reticulum lumen.	6	8	12/6
Mannosyl oligosaccharide glucosidase (MOGS)	Cleaves distal glucose from mannosyl-oligosaccharide of glycoproteins	3	5	7/3
Protein disulfide isomerase A3 (ERp57 or PD1A3)	Catalyzes rearrangement of disulfide bonds.	4	9	6/4
Extended synaptotagmin-2 (E-Syt2)	Tethers ER to cell membrane.	3	4	6/3
ER membrane protein complex subunit 1 (EMC1)	Protein folding	4	7	4/0
DnaJ homolog subfamily C member 10 (DNAJC10 or ERdj5)	ER disulfide reductase involved in disulfide rearrangement and degradation of missfolded proteins.	3	5	3/3
Dolichyl-diphosphooligosaccha	Subunit of the N-oligosaccharyl transferase	1	2	3/1

Protein	Function	Unique Peptides	% Coverage	tet/ notet
ride protein glycosyltransferase subunit 1 (RPN1)	(OST) complex which catalyzes the transfer of a high mannose oligosaccharide to glycosilated proteins.			
Protein disulfide isomerase A4 (ERp72 or PDIA4)	Catalyzes rearrangement of disulfide bonds.	3	6*	3/0
Glucosidase 2 subunit beta (GLU2B)	N-glycan processing	3	7	3/0
Protein disulfide isomerase (PDIA1)	Catalyzes the formation, breakage and rearrangement of disulfide bonds.	2	8	2/2
UDP glucose:glycoprotein glucosyltransferase 2 (UGGT2)	Reglucosidates glycoproteins with minor folding defects.	1	1	2/0
Protein sel-1 homolog 1 (Sel1L)	Involved in ER-associated degradation (ERAD)	1	3	1/0
Protein disulfide isomerase A6 (ERp5 or PDIA6)	Catalyzes rearrangement of disulfide bonds.	1	3	1/1
Coatomer subunit beta (COPB1)	Essential for the retrograde Golgi-to-ER transport of dilysine-tagged proteins	1	1	1/0
Exostosin-2 (EXT2)	Protein glycosilation	1	1	1/0
Thioredoxin	Protein reduction by thiol-disulfide exchange.	1	9	2/1

Table 3.2 Mass spectrometry candidates from pBpa crosslinking.

				Bottom	Top
Protein	**Function**	**Unique Peptides**	**% Coverage**	**pBpa/ DMSO**	**pBpa/ DMSO**
Endoplasmin	Protein folding and ERAD.	7	10	7/0	7/1
Protein disulfide isomerase A4 (ERp72 or PDIA4)	Catalyzes rearrangement of disulfide bonds.	2	5		2/0
78 kDa glucose-regulated protein (GRp78 or Bip)	Protein folding and ERAD	6	16	14/6	9/4
Dolichyl-diphosphooligosacch-aride protein glycosyltransferase subunit 1 (RPN1)	Subunit of the N-oligosaccharyl transferase (OST) complex which catalyzes the transfer of a high mannose oligosaccharide to glycosilated proteins.	3	6		3/0
Calnexin	Assist protein assambley or ER-retention of missfolded proteins.	1	3	1/1	1/1
Lipase maturation factor 1 (LMF1)	Nessesary for the maturation of dimeric lipases in the ER.	3	6	10/3	9/2
Glucosidase 2 subunit beta (GLU2B)	Glycan processing	3	6		3/0
Protein disulfide isomerase (PDIA1)	Catalyzes the formation, breakage and rearrangement of disulfide bonds.	5	11	5/0	6/0
Protein disulfide isomerase A3 (ERp57 or PD1A3)	Catalyzes rearrangement of disulfide bonds.	5	10	5/0	7/0
ERO1-like protein alpha (Ero1α)	Oxidoreductase	1	3	1/0	2/0
Zinc transporter SLC39A7	Zinc transport from the endoplasmic reticulum/Golgi apparatus to the cytosol.	2	3		2/0
Calreticulin	Chaperone that promotes folding, oligomeric assembly and quality control in the ER.	2	5	2/0	3/0
Protein disulfide	Catalyzes	1	3		1/0

				Bottom	Top
Protein	**Function**	**Unique Peptides**	**% Coverage**	**pBpa/ DMSO**	**pBpa/ DMSO**
isomerase A6 (ERp5 or PDIA6)	rearrangement of disulfide bonds.				
ER resident protein 44 (ERp44)	Oxidative protein folding.	2	5		2/0
Serpin H1	Chaperone that binds to collagen.	2	5	2/0	
Peptidyl-prolyl cis-trans isomerase B (PPIaseB)	Catalyzes the cis-trans isomerization of proline.	2	9	2/0	4/0
Ras related protein Rab-1A	RAB1A regulates vesicular protein transport from the ER to the Golgi and on to the cell surface	3	18	3/0	
Peptidyl prolyl cis-trans isomerase A (PPIA)	Catalyzes the cis-trans isomerization of proline.	4	28	4/0	4/0
Peptidyl-prolyl cis-trans isomerase FKBP1A	Catalyzes the cis-trans isomerization of proline.	1	12		1/0
Thioredoxin	Protein reduction by thiol-disulfide exchange.	2	21	2/0	2/0

Our list was enriched in proteins involved in the processing of N-linked glycans and disulfide bonds; the following proteins were of particular interest and thus selected for further study. Four PDI family members with active thioredoxin-like domains were present in our crosslinking experiments: PDI, ERp44, ERp72, and ERdj5. The PDI family is a family of 21 related mammalian proteins with at least one active thioredoxin-like domain that mediates thiol-disulfide exchange although some family members have only inactive thioredoxin-like domains[133,134]. PDI is the most predominant ER-resident PDI. It assists with disulfide bond formation, its capable of nonspecific peptide binding, and has chaperone functions[135]. *In vitro* experiments show that PDI is capable of refolding a denatured protein that lacks disulfide bonds[136]. ERp44 is important in thiol-mediated retention, a system in which monomers destined for oligomeric complexes are retained in the ER until they are properly incorporated into higher order structures[137]. ERp44 is also involved in the quality control of oligomeric proteins containing disulfide bonds[138]. ERp72 is a PDI with narrow substrate specificity[139,140]. ERp72 specializes in processing proteins like LPL that have with multiple disulfide bonds and that form parts of oligomeric complexes. ERdj5 accelerates ER associated protein degradation (ERAD) by reducing misfolded proteins, and facilitates efficient protein folding by reducing non-native disulfides[141,142]. Lastly, we are interested in the glucosyltransferases UGGT1 and 2. UGGT2 is an isoform of the better-characterized UGGT1 but both proteins localize to the ER lumen where they selectively reglucosylate unfolded glycoproteins thus playing a role in ER quality control[143].

Knockdown of Candidate LMF1-interacting Partners Reduces LPL secretion

We next tested the role of our novel LMF1 binding partners in LPL secretion. PL, which does not depend on LMF1 for exit from the ER, served as a negative control for changes to the ER protein-folding environment. siRNAs against ERp44, PDI, ERp72, UGGT2, ERdj5 and UGGT1 were compared to a scrambled siRNA control (NC). As shown in the media fraction of **Figure 3.3A-B**, knockdown of ERp44, ERp72, UGGT2, and ERdj5 decreased secretion of LPL much more dramatically than PL. Knockdown of UGGT1 slightly decreased LPL, but not PL, secretion. Unexpectedly, knockdown of PDI seemed to increase secretion of both LPL and PL. The knockdown of the LMF1 interacting partners was measured in the lysate fraction (**Fig. 3.3A-B**), and for most partners knockdown was similar for LPL and PL, as shown in **Figure 3.3C**.

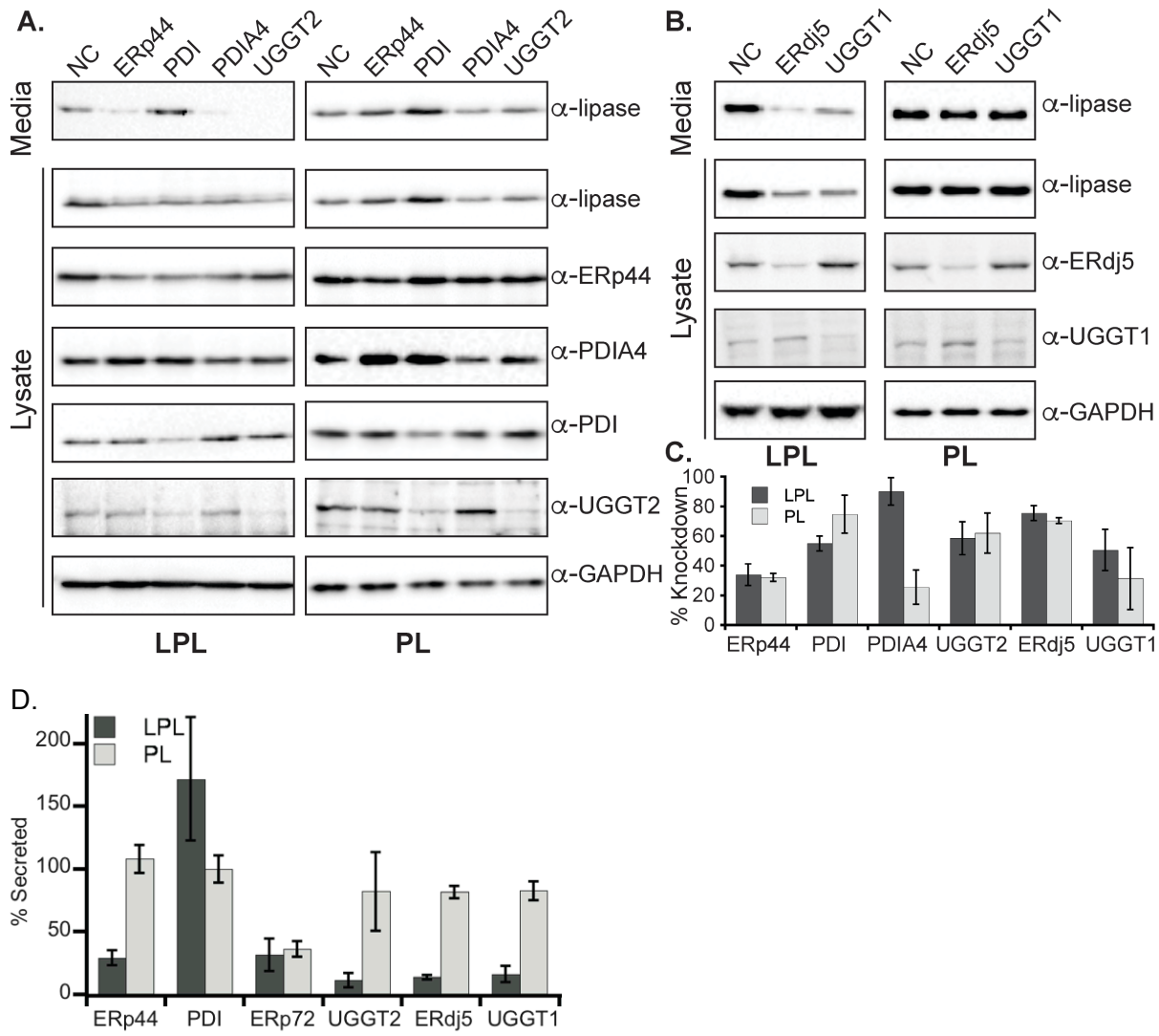

Figure 3.3 siRNA knockdown of novel LMF1-interacting partners affects LPL secretion.

A) and B) HEK293 cells stably expressing LPL-V5 or PL-V5 were transfected with scrambled siRNA (NC) or siRNA against the newly identified LMF1-interacting partners. Lipase secretion into the media was induced with heparin, and media and lysate fractions were collected for analysis. Media fractions were probed with 41a antibody for LPL and a C-terminus V5 tag for PL. Lysates were also probed for the respective LMF1 interacting-partners. GAPDH was used as a loading control. C) siRNA knockdowns shown in A and B were performed in triplicate. The intensity of bands for each knocked down protein was quantified using Image Lab, and the percent knockdown was calculated as described in methods. D) Quantification of lipase secretion normalized to the cell number per sample and to secretion with scrambled siRNA. Just like for panel C, band intensity was quantified with Image Lab and error bars indicate the standard error.

Novel Partners form Complexes with LMF1 and LPL

We next set out to determine if the novel LMF1 partners would bind to LMF1, LPL, or both. We first purified LMF1 via the His tag after in-cell crosslinking with DSP to binding partners. We then performed Western Blots against the interacting partners to determine if there was an increase in the apparent molecular weight of the partners in samples not treated with DTT. We next treated samples with DTT and looked for bands that collapsed down to the expected molecular weight. ERp44, UGGT2 and ERp72 form higher-molecular weight complexes with LMF1 when crosslinked with DSP, as shown in **Figure 3.4**, LMF1 panel. Blots were stripped and re-probed using α-His antibody to ensure that the complexes contained LMF1 (not shown). We repeated these experiments but replaced His-tagged LMF1 with LPL. We found UGGT2, PDI and ERp72 in a high molecular weight complex with LPL which was also affinity purified via a His tag. **Table 3.3** summarizes these results as well as other ER resident candidates that according to our findings do not interact with LMF1 or LPL. A horizontal line denotes a condition we did not tested for.

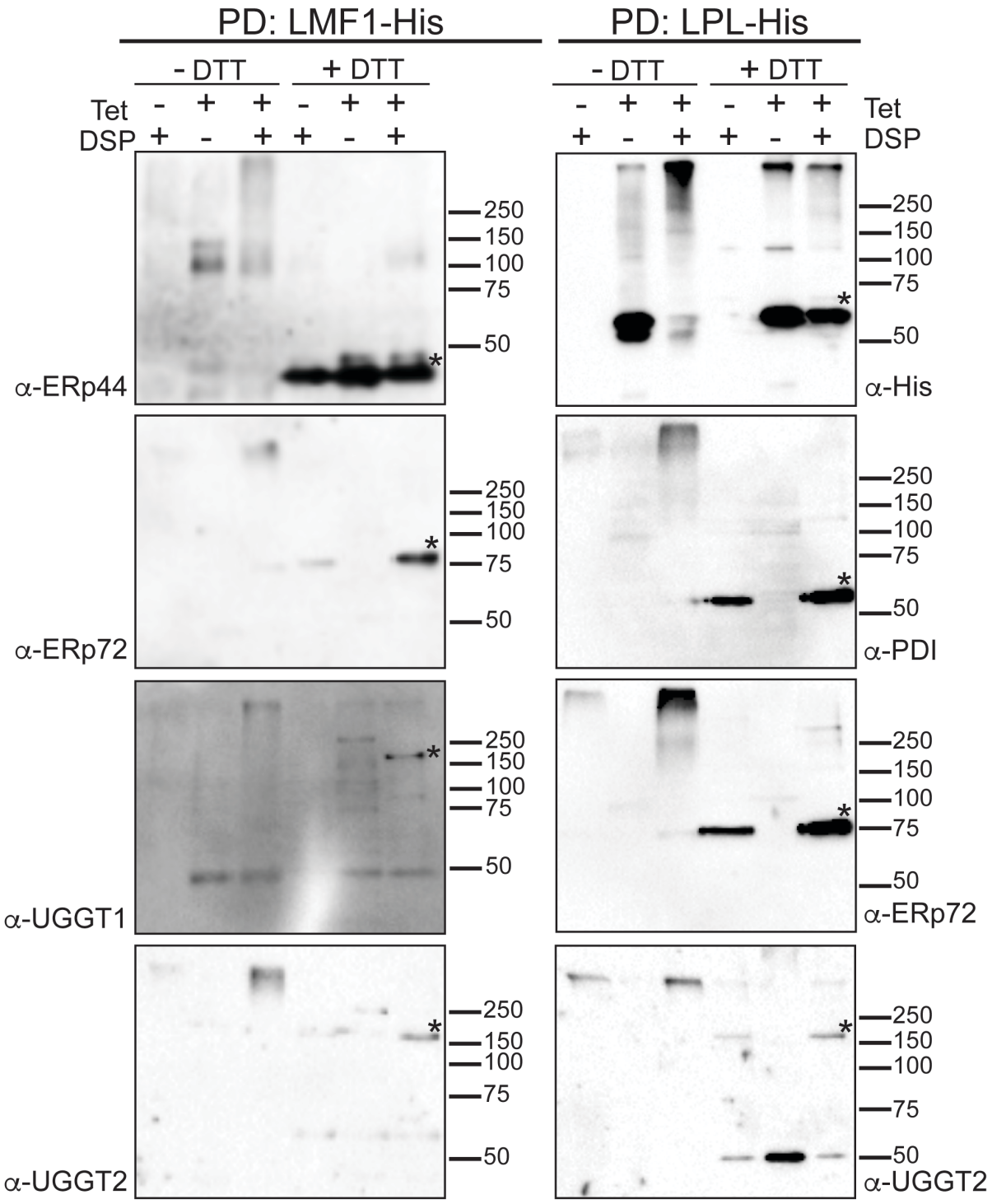

Figure 3.4 Validation of novel LMF1 and LPL interacting partners.
Cells stably expressing LMF1-His or LPL-His were induced with tetracycline followed by treatment with DSP crosslinker. The His-tagged protein was purified and then samples were probed for the indicated interacting partner. A) Pull downs of LMF1-His show that LMF1 interacts with ERp44, ERp72, UGGT1, and UGGT2. B) Pull downs of LPL-His show that LPL interacts with PDI, ERp72, and UGGT2.

Table 3.3 Summary of pull down results for both crosslinkers and LPL secretion studies.

	DSP		pBpa	siRNA
Protein Candidate	**LMF1-His**	**LPL-His**	**LMF1 loop C**	**Hinders LPL secretion**
ERp44	yes	no	yes	yes
ERp72	yes	yes	no	yes
UGGT1	yes	no	-	yes
UGGT2	yes	yes	-	yes
ERdj5	no	no	-	yes
Bip	no	no	no	-
Ero1-α	no	no	no	-
Endoplasmin or GRp94	no	no	no	-
PDI	no	yes	no	no
ERp57	-	no	no	-

ERp44, ERdj5 and TRX form Thiol-dependent complexes with LMF1

Unexpectedly, we saw higher molecular weight bands in the ERp44-LMF1 samples in the absence of DSP (**Fig. 3.4**, LMF1-ERp44 panel, + Tet, - DSP, -DTT lane). This clue suggests that LMF1 might play an important role in cellular redox homeostasis. Because DSP crosslinks can be broken through the addition of a reducing agent, we used non-reducing loading buffer for our crosslinked samples prior to SDS-PAGE. When we used a reducing loading buffer, DSP-independent ERp44-LMF1 complexes were lost (**Fig. 3.4**, LMF1-ERp44 panel, + Tet, - DSP, + DTT lane). We thus set out to determine if any other LMF1-binding partners formed thiol-dependent complexes with LMF1. To do so we collected cells expressing LMF1-His, and quenched disulfide exchange in the cells with trichloroacetic acid (TCA) and the addition of N-Ethylmaleimide (NEM). We purified the complexes via LMF1's His tag and ran non-reducing gels for Western blots. We probed for the oxidoreductases listed in **Table 3.3**. We also checked the list of proteins identified by mass spectrometry for additional redox active proteins. One cytosolic protein, TRX was not initially tested because we focused on ER-resident proteins. The unique peptide counts as well as percent coverage for TRX is included at the end of **Tables 3.1** and **3.2**. Westerns for TRX were also performed. We found thiol-dependent bands with molecular weights corresponding to the protein of interest plus LMF1 using antibodies against ERp44, TRX, and ERdj5 (**Fig. 3.5A,** arrows indicate expected molecular weight in lysates and asterisks indicate complexes). We did not find ERdj5 in a complex with LMF1 when cells were treated with DSP. This may be because DSP could crosslink other more abundant proteins and block ERdj5-LMF1 interactions.

Because we found ERdj5, ERp44 and TRX in thiol-dependent complexes with LMF1, we wanted to determine which cysteines on LMF1 are important for its function. LMF1 has several highly conserved cysteines. We mutated cysteines at position 145, 231, 237, 288, 322, 445, and 453 to alanines by site-directed mutagenesis. The positions of these cysteines on LMF1 are shown in **Figure 3.5B**. We also made a complete cysteine mutant, and two compound mutations with both membrane cystines (245, 288) and both C-terminal cysteines (445, 453) mutated to alanines. These cysteine mutant LMF1 constructs were transfected into *cld/cld* mouse embryonic fibroblasts (MEFs) along with a plasmid expressing LPL-V5. These MEFs are derived from mice homozygous (*cld/cld*) for the combined lipase deficiency mutation, which is a truncation mutation in LMF1[77,81]. WT LMF1 and a plasmid expressing GFP served as positive and negative controls, respectively. All mutations reduced LPL secretion relative to WT LMF1 (**Fig. 3.5C**, media panel). The effects were most severe at positions 237, 288, 322, 445, 453 and the compound and complete mutations. However, no LMF1 expression was observed when LMF1 was mutated at position 237 or at all of the cysteines (**Fig. 3.5C**, α-LMF1 panel). Thus, positions 288, 322, 445 and 453 seem to be particularly important for LPL secretion.

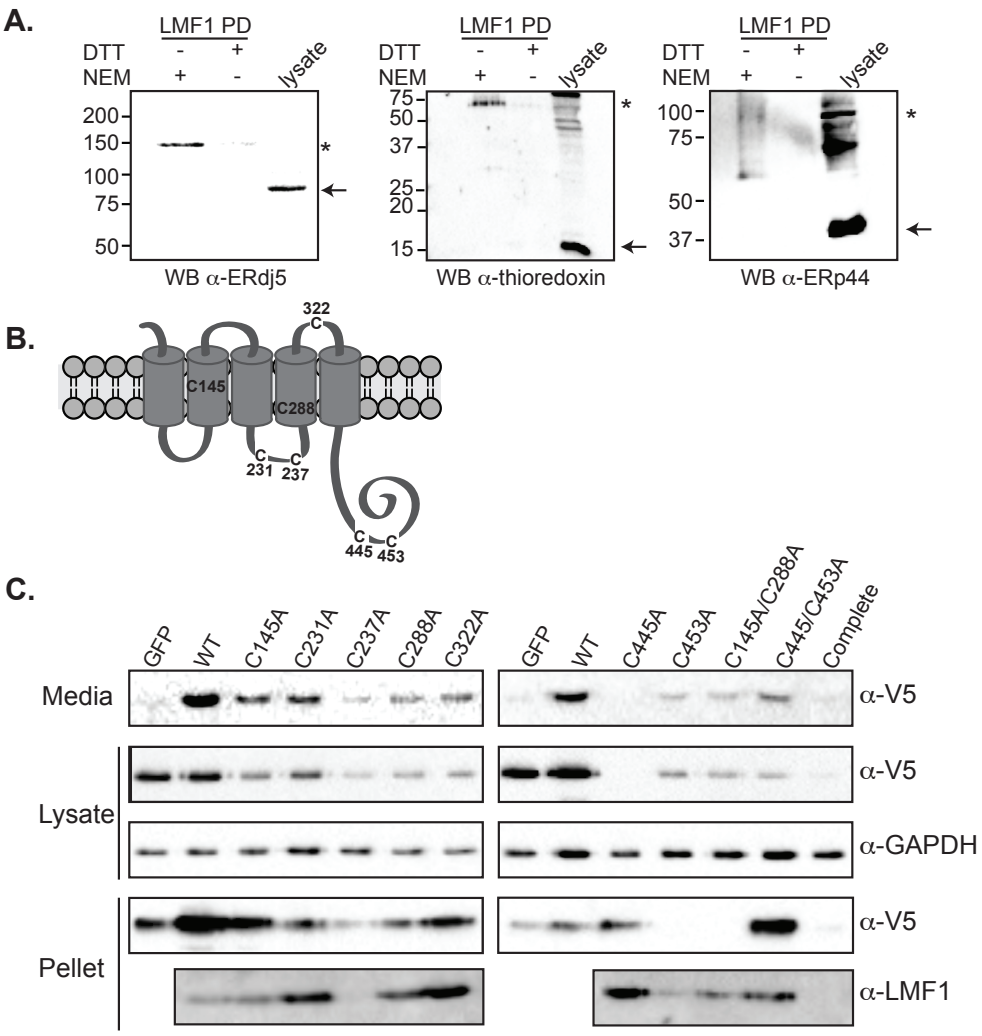

Figure 3.5 ERp44, ERdj5 and TRX interact with LMF1 in a thiol-dependent manner. A) NEM addition stabilizes mixed disulfides of LMF1 with ERdj5, TRX, and ERp44. LMF1-His was purified from TCA precipitated cell lysate treated with NEM, then samples were probed using antibodies against the indicated interacting partners. Cells treated with DTT served as a control. B) Schematic of the membrane topology of LMF1 and the location of the conserved cysteine's tested. C) Secretion of LPL-V5 from *cld/cld* cells transiently transfected with LMF1 bearing the indicated cysteine to alanine mutations. Lipase levels in the lysate and pellet, and LMF1 levels in the pellet, are also probed. GAPDH serves as a loading control. The data for Figure 3.5C was provided by Lindsey J. Broadwell.

Levels of Cytosolic TRX Influence LPL, but not PL, secretion

Because we found TRX in a thiol-dependent complex with LMF1, we reduced its cellular levels using siRNA and tested for effects on LPL secretion. As shown in **Figure 3.6A**, media panel, reduction of cellular TRX dramatically reduced LPL secretion. However, PL secretion was not affected. We also overexpressed thioredoxin-interacting protein (TXNIP). TXNIP binds reduced TRX through disulfide linkages and inhibits TRX activity[144]. When TXNIP is overexpressed, LPL, but not PL, secretion is severely reduced (**Fig. 3.6B**, media panel and TXNIP panel). Thus, TRX is not only in a complex with LMF1 but is also required for robust LPL secretion. In combination with the data from **Figure 3.5**, these data suggest that LMF1 may connect cytosolic thioredoxin with ER-resident oxidoreductases.

To further probe this connection we next compared sensitivity of *cld/cld* and *cld/wt* (heterozygous littermates) MEFs to a series of drugs that perturb cellular redox homeostasis and protein folding. These drugs were buthionine sulfoximine (BSO), dithiothreitol (DTT) and tunicamycin. BSO inhibits synthesis of the reducing agent glutathione[145]. If LMF1 transfers reducing equivalents to the ER, we would expect *cld/cld* cells to be more sensitive to BSO than *cld/wt* cells. Tunicamycin blocks N-linked glycosylation thus causing an accumulation of unfolded glycoproteins in the ER, which induces the unfolded protein response (UPR)[146]. Many of these unfolded proteins are destined for ERAD, and thus tunicamycin should increase the demand for ERdj5 to reduce their disulfide bonds[142]. If LMF1 contributes to reduction of ERdj5, cells lacking LMF1 should be hypersensitive to tunicamicyn. As a strong reducing agent, DTT blocks disulfide bond formation. If LMF1 provides reducing equivalents, we would not expect

cld/cld cells to be more sensitive to DTT than *cld/wt* cell. As shown in **Figure 4C**, we found that relative to *cld/wt* cells, *cld/cld* cells were slightly more sensitive to BSO and dramatically more sensitive to tunicamycin. However, *cld/wt* and *cld/cld* cells were equally sensitive to DTT.

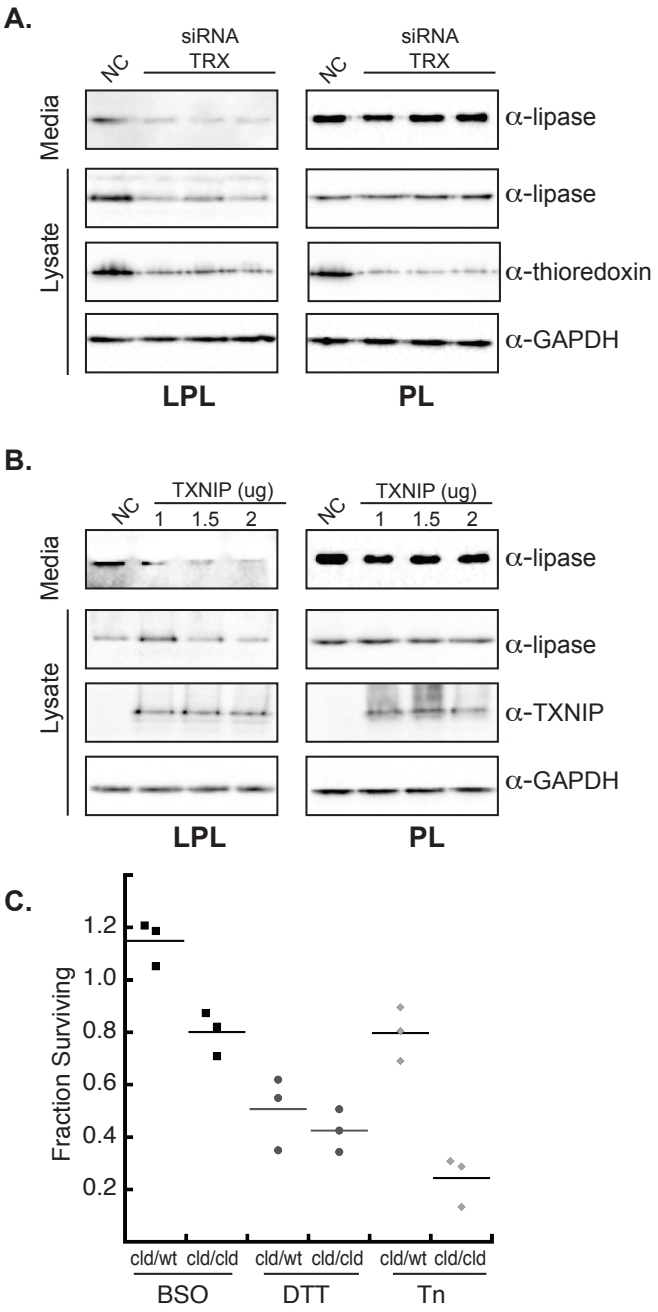

Figure 3.6 Cellular TRX levels and activity affect LPL, but not PL, secretion. A) HEK293 cells stably expressing LPL-V5 or PL-V5 were transfected with scrambled siRNA (NC) or siRNA against TRX. Lipase and TRX levels were tested in the media and lysate fractions as described in Fig. 3. B) TXNIP overexpression in HEK293 cells stably expressing LPL-V5 or PL-V5 hinders secretion of LPL, but not PL. C) MEFS homozygous (*cld/cld*) or heterozygous (*cld/wt*) for a loss of function mutation in LMF1 were treated with BSO, DTT, or tunicamycin (Tn). Treated cell and untreated cells were counted, and the percent of surviving cells was calculated. The difference between survival *cld/cld* and *cld/wt* cells for BSO and tunicamycin treatment were statistically significant as determined by a 2-tailed student's t-test ($p < 0.05$). Survival of *cld/cld* and *cld/wt* cells treated with DTT was not significantly different ($p > 0.05$).

Discussion

Our goal was to understand how LMF1 promotes LPL maturation. From our lipase chimeras we learned that the C-terminus of LPL is important for LPL's secretion and that only the C-terminus of LPL interacts physically with LMF1. From our mass spectrometry data we derived a role for LMF1 in ER redox homeostasis. Through our mixed disulfide and DSP crosslinking experiments we found five novel, ER-resident binding partners of LMF1 (ERp44, ERp72, ERdj5, UGGT1, and UGGT2). Protein downregulation via siRNA validates the requirement of these five candidates for LPL secretion. ERp44 reduces oxidized subunits of proteins such as adiponectin destined to assemble into higher molecular weight complexes[147]. ERp44 also uses a thiol linkage to retrieve Golgi-localized orphan subunits of proteins (such as IgM) intended for disulfide-linked oligomers back to the ER[148]. The disulfide bond between ERp44 and the orphan subunit must then be reduced. ERdj5 is known to reduce disulfide bonds for proteins destined for ERAD as well as nonnative disulfides required for the productive folding of substrates such as the LDL receptor[141,142]. ERdj5's thioredoxin domain has the lowest reduction potential among the PDI family, and hence can reduce other PDIs but can't be reduced by them[149]. The mechanism by which ERdj5 is reduced once its active site is oxidized is unknown, but it has been suggested that ERdj5 could be reduced by glutathione or other small redox cofactors[141,149]. We suggest that LMF1 facilitates the reduction of these proteins, resolving these outstanding mysteries.

We also found an important role for cytosolic thioredoxin in LPL secretion. First, we detect the formation of a mixed disulfide bond between LMF1and TRX. Aditionally, TRX downregulation via siRNA as well as inhibition of cytosolic TRX by overexpression

of TXNIP decreases secretion of LPL. These data suggest that LMF1 provides a physical and functional linkage between cytosolic TRX and ER-resident oxidoreductases. LMF1 thus resembles DsbD, the bacterial periplasmic protein that transfers electrons from cytosolic TRX to substrates in the periplasm. DsbD has no known homologue in eukaryotes, and it was widely assumed that glutathione powered disulfide reduction in the ER[150]. However, a recent study showing that depletion of ER-resident glutathione had no effect on disulfide bond isomerization, the reduction-dependent degradation of ERAD substrates, or the induction of the UPR[151]. These data led the authors to conclude that an alternative small molecule or a eukaryotic homologue to DsbD was responsible for providing reducing equivalents to oxidoreductases in the ER[151].

We propose that although LMF1 was not previously recognized to have a role in redox homeostasis in the ER, it fills this role. This role for LMF1 was not readily apparent because although our data shows that LMF1 has strong functional homology to DsbD, the two proteins have only weak sequence homology. Unlike DsbD, LMF1 is not annotated as containing a thioredoxin-like domain. LMF1's conserved cysteines are not arranged in a canonical C-X-X-C motif. However, a pairwise alignment of LMF1 and DsbD revealed a stretch of about 100 amino acids in the C-terminus of both proteins with 23% sequence identity (**Fig. 3.7**). This is the C-terminal ER/periplasmic region of both proteins and contains residue C453 of LMF1 and the final redox-active cysteine pair of DsbD. Perhaps LMF1 keeps ERdj5 in a reduced state to promote isomerization of non-native disulfide bonds on LPL in a manner similar to DsbD reduction of DsbC to promote disulfide isomerization in prokaryotes. At this time we do not know if LMF1

uses a cysteine relay similar to DsbD, and will resolve its mechanism of action through future studies.

However, analysis of LMF1-related proteins supports the idea that, like DsbD, it uses some mechanism for transmembrane electron transport. The protein family database, or Pfam, groups proteins into families based on sequence alignments and a profile hidden Markov model (HMM) analysis. Related families are grouped into clans, which are families with sequence, structure, or profile-HMM similarity[152]. LMF1 belongs to a clan that includes the archaeal and bacterial membrane proteins DoxD, DoxX, and MauE. Strikingly, these three transmembrane proteins are all involved in redox reactions. DoxD is a multipass membrane protein that, with its binding partner DoxA, oxidizes thiosulfate to reduce quinone[153]. DoxX is a recently identified *Mycobacterium tuberculosis* multipass membrane protein that forms a complex with SodA and SseA to link detoxification of superoxide radicals generated during the phagocyte oxidative burst with cytosolic thiol homeostasis[154]. MauE is a multipass membrane protein from *Paracoccus denitrificans.* MauE and its partner, MauD, are involved in the oxidation of methylamine[155].

We propose that LMF1 may be part of a center for folding disulfide bond-containing proteins that are functional as oligomers, such as LPL. First, these proteins may have a special need for reduction of mispaired disulfide bonds to allow additional rounds of folding. Next, many secreted proteins have both N-linked glycans and disulfide bonds, and processing of these two postranslational modifications are intimately linked[156]. We found peptides specific to both UGGT1 and UGGT2 in our analysis of LMF1-binding partners. UGGT1 is a glucosyltransferase that functions in ER

quality control of glycoproteins, but the function of UGGT2, an isoform of UGGT1, is still a subject of debate[143]. UGGT1 acts after the initial processing of an N-linked oligosaccharide. If the glycoprotein has not achieved its native conformation, the glucosyltransferase UGGT1 aids in folding by adding back a glucose residue, allowing another round of association with calnexin and calreticulin[143]. Although some studies have concluded that UGGT2 is enzymatically inactive[143,157], other studies show that it has glycosyltransferase activity when tested on a synthetic substrate[158]. Additionally, studies in *C. elegans* showed that the two isoforms played different roles in response to ER stress[159]. We found that siRNA knockdown of both UGGT1 and UGGT2 resulted in loss of LPL secretion, but the effect was more pronounced for UGGT2. LPL is thus the first known physiological substrate for UGGT2. Intriguingly, UGGT2 is expressed in heart and skeletal muscle, an expression profile similar to LPL[143]. We also found UGGT2 in a complex with LMF1. These data lead us to speculate that UGGT2 may partner with LMF1 to assist in the folding of secreted, disulfide rich, oligomeric glycoproteins.

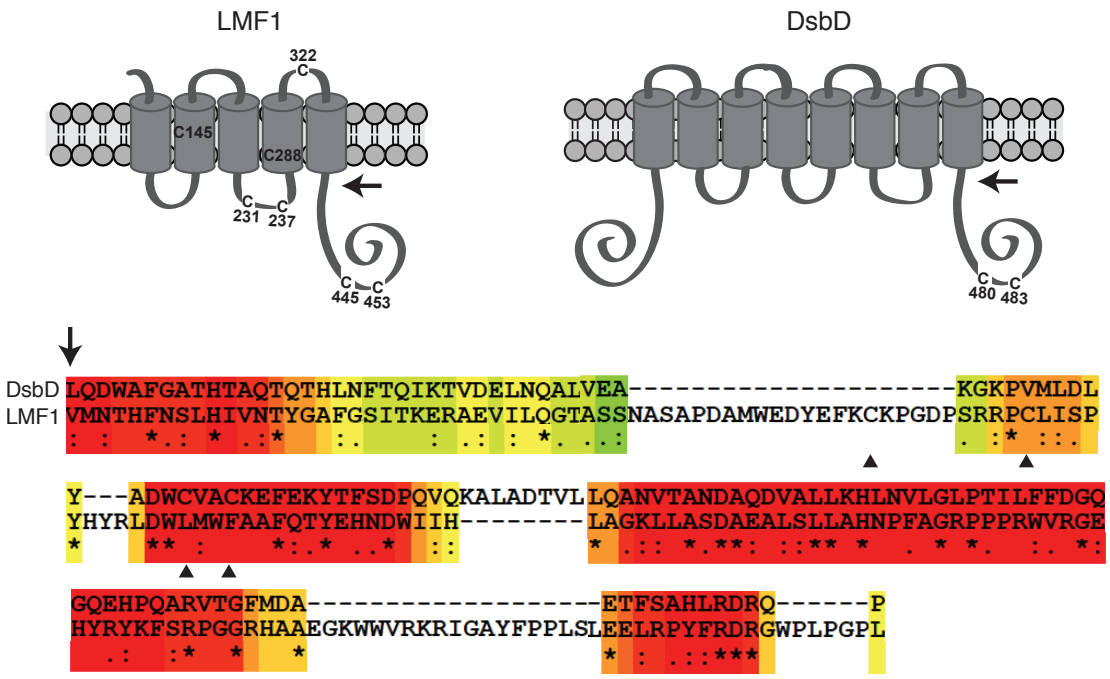

Figure 3.7 Schematic of LMF1 and DsbD.
A pairwise alignment was performed using Tcoffee. The C-terminal ER or periplasmic region of the two proteins was 23% identical. Conservation starting after the last transmembrane segment is shown. Red represents good conservation and green represents poor conservation. Key cysteines are marked with a triangle.

CHAPTER 4: CONCLUSIONS AND FUTURE DIRECTIONS

Introduction

This thesis work provides data that has shed light on the role of LMF1 in dimeric lipase maturation. We learned from the N-terminal domain truncations of LMF1 that full length FL LMF1 is necessary for the maturation of LPL. Our studies with the lipase chimeras show that the C-terminus of LPL is important for LPL's secretion. Furthermore, our crosslinking pulldowns revealed that the C-terminus of LPL interacts with LMF1 thus we have narrowed down the site of interaction of LMF1 on LPL. However, the mechanism by which LMF1 is retained in the ER remains unknown. We found protein-protein interactions between LMF1 and ERp44 with different crosslinkers (**Table 3.3**) plus mixed disulfide formation from the NEM studies (**Fig.3.5A**). ERp44 is known to participate in thiol-mediated retention in the ER eukaryotes. The oxidoreductase Ero1-α lacks an ER retention signal but Ero1-α is retained in the ER though a mixed disulfide with ERp44[160]. LMF1 also lacks a known ER retention signal, thus we used siRNA against ERp44 and the ER marker Sec16 to determine if ERp44 helps to retain LMF1 in the ER. However, downregulation of ERp44 does not hinder the ER localization of LMF1 (**Figure 4.1**).

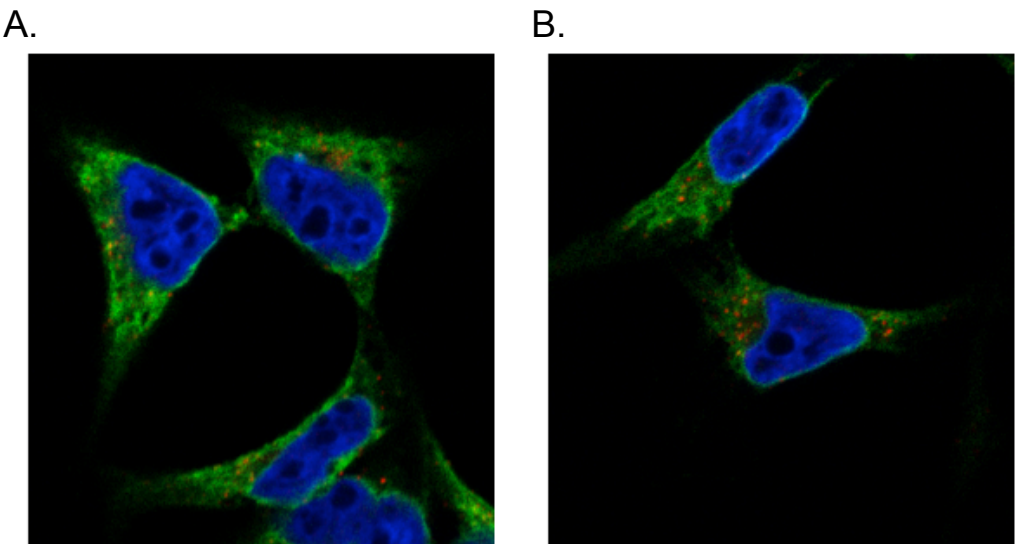

Figure 4.1 ERp44 is not responsible for ER retention of LMF1.
A) LMF1-His HEK293 cells transiently transfected with: A) scrambled siRNA as negative control (NC) or B) 20 nM of siRNA against ERp44. The merged images are shown, LMF1 is represented in green while Sec16 is red. After 24 hrs post-siRNA transfection, the cells were induced with 1 ug/mL of tetracycline. Cells were fixed with 4% paraformaldehyde 48 hrs post-transfection and permeabilized with 0.1% triton X-100. Sec16 antibody was used at 1:100 and anti-His at 1:200 with Alexa Fluor 594 (1:500) and 488 (1:800) respectively for fluorescence detection.

An early hypothesis for how LMF1 promotes lipase maturation was that LMF1 acts as a cargo receptor for dimeric lpases. Homozygous LMF1 mutations in patients result in low plasma levels of dimeric lipases. This phenotype is reminiscent of other disorders resulting from mutations in cargo receptors. For example, patients with a rare inherited bleeding disorder (Factor V/VIII deficiency) have low plasma levels of factor V and VIII due to mutations in one of two proteins that form a cargo receptor complex in the ER[161]. A special client-specific cargo receptor is needed for incorporation of the coagulation factors into COPII vesicles for proper incorporation in the secretory pathway. To investigate if LMF1 is a cargo receptor required for ER exit of dimeric lipases, we used immunofluorescence to determine if LMF1 localizes to COPII vesicles. Sec16, a common COPII vesicle marker, has a punctate pattern characteristic of COPII vesicles (**Fig. 4.2,** second panel)[162]. However, LMF1 shows a tubular pattern characteristic of other chaperones such as GRP78, calnexin, and calreticulin that localize to the peripheral ER (**Fig. 4.2**, third panel)[81]. Based on the distinct expression patterns of LMF1 and Sec16 we concluded that LMF1 is not a cargo receptor.

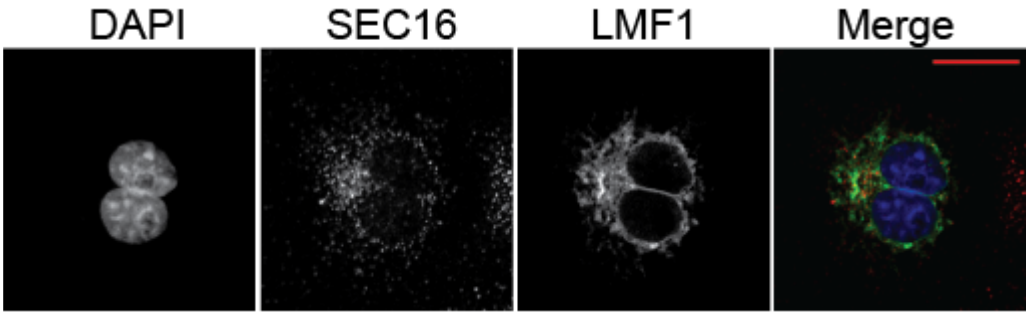

Figure 4.2 LMF1 does not localize to ER exit sites.
Immunofluorescence of LMF1 with the COPII marker Sec-16 in COS-7 cells. Scale bar represents 20 μm. LMF1 and Sec16 were detected as in **Figure 4.1**.

Our most interesting finding was the discovery of novel interacting partners of LMF1 that are essential for LPL secretion and that have revealed a role in ER-redox homeostasis for LMF1. We report LPL as the first known physiological substrate for UGGT2. Additionally, we found redox-active proteins among the novel-binding partners of LMF1. These redox-active proteins are the cytosolic thioredoxin (TRX) and the ER resident proteins ERp72, ERp44, and ERdj5. Sequence alignment of LMF1 across species reveals that LMF1 has several conserved cysteines (**Fig. 4.3**) of which we found positions 288, 322, 445, and 453 to be needed for LPL secretion. Similarly, DsbD has three domains, each with a conserved pair of reactive cysteines important for the electron transfer from cytosolic TRX[163]. Furthermore, alignment of the C-terminal/periplasmic region of LMF1 and DsbD respectively contains a stretch of about 100 amino acids with 23% sequence identity (**Fig. 3.7**). Our findings lead us to propose that LMF1 is also a transmembrane electron transporter like DsbD thus it promotes protein folding by connecting cytosolic TRX to ER-resident oxidoreductases such as ERp72, ERp44, and ERdj5.

Why full length is required for lipase maturation remains unanswered. The cysteines important for LPL maturation are in the DUF122 domain[81,84,117]. The DUF122 domain was already known to be important for dimeric lipase maturation. We also know that loop A is not required for LPL binding[82]. Perhaps loop A is needed for ER-retention of LMF1 or for protein-protein interactions with one of our novel LMF1 binding partners that reside in the ER lumen.

Figure 4.3 Sequence alignment of LMF1 reveals cysteine conservation.
Red arrows denote nine conserved cysteines of LMF1. We performed point mutations in all of them (data not shown for C87) except for 188 but only saw an inhibitory secretion effect for LPL with the cysteines in positions 288, 322, 445, and 453. These cysteines localize to the DUF1222 domain of LMF1 (for the topology of LMF1 see **Fig. 1.3**). This sequence alignment was performed using Clustal Omega.

Future directions

Confirming the role of LMF1 in electron transfer

I have generated HEK293 stable cell lines expressing point mutations of cysteines to alanines in the four cysteines important for LMF1 function (288, 322, 445, and 453). Position 322 is exposed to the cytosol so we have hypothesized this cysteine is crucial for formation of the mixed disulfide bond with TRX. Alternatively, DsbD transfers the two electrons across the cytoplasmic membrane by a pair of cysteines that are predicted to be within the transmembrane segments[164]. Thus C288 of LMF1 could be the cysteine that forms a mixed disulfide bond with TRX. Positions 445 and 453 localize to the C-terminal domain of LMF1 which faces the ER-lumen thus we have hypothesized these two residues can form mixed disulfide bonds with ERp44 or ERdj5. We will determine if our mutants abolish the formation of these mixed disulfide bonds by adding the alkylating agent NEM to cell lysates from the stable cell lines expressing the point mutations of LMF1.

Based on the formation of mixed disulfides between LMF1 with TRX and ERdj5, we hypothesized that LMF1 maintains ERdj5 in a reduced state to promote isomerization of non-native disulfide bonds on LPL in eukaryotes. This role for LMF1 would be similar to the role of DsbD in reducing DsbC in prokaryotes and ERdj5 would participate in isomerization of disulfide bonds. An *in vitro* experiment with purified LMF1, TRX, LPL and PDIs can further our understanding of the role of LMF1 in redox homeostasis within the ER as well as the role of the three PDIs we detected as novel interacting partners of LMF1. LMF1 can be purified from SF9 cells as we have done previously[165]. Since LMF1 is a five segment transmembrane protein, phospholipid

bilayer nanodiscs will be used to prevent aggregation and provide a more physiological environment[166,167]. LPL can be purified from bovine milk[168] and denatured with guanidinium hydrochloride to study the folding effects of the PDIs. LPL folding can be assessed by the measurement of LPL activity using a fluorescent triglyceride analogue[169]. Experiments can be performed with LPL, LMF1, a PDI and with/without TRX. If TRX addition promotes LPL folding significantly with PDI addition, we can conclude that LMF1 transfers electrons from TRX to the PDIs. Further more, by adding ERp72, ERdj5, and ERp44 separately we can determine which is the primordial PDI required for proper folding of LPL.

To determine if there is electron transfer due to disulfide bond oxidation and reduction, LMF1 can be separated into domains containing cysteine pairs and expressed simultaneously similar to what was done with DsbD when determining that the electron transfer occurs via a disulfide bond cascade[170]. LMF1 can be separated into two pieces taking into consideration that all the cysteines of LMF1 important for LPL maturation are in the DUF122 domain. These pieces are a C-terminal truncation containing the first four transmembrane domains of LMF1 and an N-terminal truncation containing the C-terminal soluble domain, which harbors a cysteine pair. The ER retention signal used previously will be added to the C-terminal truncation[165]. Each segment of LMF1 must contain a different tag so the oxidation state of each segment of LMF1 can be assessed as was done for DsbD[170]. Additionally, the cysteines not essential for LPL maturation should be replaced by alanines for each segment. Importantly, for this assay we need to determine the oxidation state of a substrate of LMF1. If ERdj5 does enhance LPL activity in the *in vitro* experiment it could be used as

LMF1's substrate. The oxidation state of ERdj5 can be determined by acid trapping cell lysates and alkylation of free cysteines with NEM. Expression of LMF1 constructs (in a knock out cell line for LMF1) will reveal the ability of LMF1 in reduction of ERdj5. A higher molecular weight band represents the reduced form of ERdj5 due to the incorporation of the alkylating agent. If the co-expression of both LMF1 segments does not restore the electron transfer activity of LMF1, there would be accumulation of ERdj5 in the oxidized state (lower molecular weight band). Conversely, if the co-expression of both segments of LMF1 restores activity, most of the ERdj5 will be detected in the reduced state. A cell line knocked out for LMF1 is required for this experiment.

Searching for other substrates of LMF1

LMF1 is ubiquitously expressed[81,86], however the dimeric lipases are not. Thus LMF1 must be important for folding other proteins in the tissues that do not express dimeric lipases. Our newly found role for LMF1 as a transporter of electrons from the cytosol to ER-resident oxidoreductases suggests that in other tissues, LMF1 is important for folding of proteins with a high number of disulfide bonds like the dimeric lipases. We have reviewed our mass spectrometry data from our DSP and pBpa crosslinking studies and selected the top 10 (by peptide count) secreted proteins identified as LMF1 binding partners (**Table 3.1**). Most the protein candidates are oligomers that are enriched in disulfide bonds. Future experiments include expression of these candidates in *cld/cld* and *cld/wt* cells to determine if they are not secreted in *cld/cld* cells due to the expression of the truncated form of LMF1.

Table 4.1 Secreted protein candidates for LMF1 substrates.

Sample	Name	Disulfide Bonds	Oligomeric State
pBpa	Fibronectin	29	dimer (ECM)/ monomer (blood)
pBpa	Aggrecan core Protein	15	heteroligomer
pBpa	Cartilage oligomeric matric protein	24	pentamer
pBpa	Hyaluronan/ proteo-glycan link protein	5	heteroligomer
pBpa	Biglycan	3	homodimer
DSP	Ig gamma-1 chain C	5	heteroligomer
DSP	Protein S100-A8	0	monomer
DSP	Capthesin D	4	heteroligomer
DSP	Ig gamma-2 chain C	2	heteroligomer
DSP	Integrin beta 1	29	heterodimer

Final remarks

LPL is the main lipase for triglyceride clearance within the capillary lumen and one third of the USA adult population has high lipid levels. Thus we sought to determine the role of LMF1 in LPL maturation. First, using a truncation approach we found that every loop of LMF1 facing the ER is necessary for the maturation process to take place. Second, crosslinking followed by proteomics and data validation revealed that LMF1 mainly interacts with proteins involved in oxidative folding. Furthermore, the utilization of drugs that modify the ER environment point towards a role in ER redox homeostasis for LMF1. Additionally, LMF1 has conserved cysteines in a similar manner than DsdD thus we have concluded that LMF1 might be the long sought for eukaryotic homologue of DsbD. As a next step, it remains to be determined if LMF1 utilizes a cysteine cascade as a means to transfer reducing equivalents into the ER lumen similarly to DsbD in prokaryotes. This newly found role for LMF1 provides an explanation for the expression of LMF1 in tissues that lack LPL and other dimeric lipases and our proteomics data has provided a starting point in the search for other substrates of LMF1.

REFERENCES

1. Hide, W.A., Chan, L. & Li, W.H. Structure and evolution of the lipase superfamily. *J Lipid Res* **33**, 167-78 (1992).

2. Doolittle, M.H., Ehrhardt, N. & Peterfy, M. Lipase maturation factor 1: structure and role in lipase folding and assembly. *Current opinion in lipidology* **21**, 198-203 (2010).

3. Semenkovich, C.F. et al. Lipoprotein lipase and hepatic lipase mRNA tissue specific expression, developmental regulation, and evolution. *J Lipid Res* **30**, 423-31 (1989).

4. Jaye, M. et al. A novel endothelial-derived lipase that modulates HDL metabolism. *Nat Genet* **21**, 424-8 (1999).

5. Wion, K.L., Kirchgessner, T.G., Lusis, A.J., Schotz, M.C. & Lawn, R.M. Human lipoprotein lipase complementary DNA sequence. *Science* **235**, 1638-41 (1987).

6. Chajek, T., Stein, O. & Stein, Y. Pre- and post-natal development of lipoprotein lipase and hepatic triglyceride hydrolase activity in rat tissues. *Atherosclerosis* **26**, 549-61 (1977).

7. Gonzalez-Navarro, H. et al. Identification of mouse and human macrophages as a site of synthesis of hepatic lipase. *J Lipid Res* **43**, 671-5 (2002).

8. McCoy, M.G. et al. Characterization of the lipolytic activity of endothelial lipase. *J Lipid Res* **43**, 921-9 (2002).

9. Ben-Zeev, O. et al. Lipase maturation factor 1 is required for endothelial lipase activity. *Journal of lipid research* **52**, 1162-9 (2011).

10. Davis, R.C. et al. Hepatic lipase: site-directed mutagenesis of a serine residue important for catalytic activity. *J Biol Chem* **265**, 6291-5 (1990).

11. Emmerich, J. et al. Human lipoprotein lipase. Analysis of the catalytic triad by site-directed mutagenesis of Ser-132, Asp-156, and His-241. *J Biol Chem* **267**, 4161-5 (1992).

12. Lowe, M.E. The catalytic site residues and interfacial binding of human pancreatic lipase. *J Biol Chem* **267**, 17069-73 (1992).

13. Wang, Z., Li, S., Sun, L., Fan, J. & Liu, Z. Comparative analyses of lipoprotein lipase, hepatic lipase, and endothelial lipase, and their binding properties with known inhibitors. *PLoS One* **8**, e72146 (2013).

14. Winkler, F.K., D'Arcy, A. & Hunziker, W. Structure of human pancreatic lipase. *Nature* **343**, 771-4 (1990).

15. Bourne, Y. et al. Horse pancreatic lipase. The crystal structure refined at 2.3 A resolution. *J Mol Biol* **238**, 709-32 (1994).

16. van Tilbeurgh, H. et al. Interfacial activation of the lipase-procolipase complex by mixed micelles revealed by X-ray crystallography. *Nature* **362**, 814-20 (1993).

17. van Tilbeurgh, H., Sarda, L., Verger, R. & Cambillau, C. Structure of the pancreatic lipase-procolipase complex. *Nature* **359**, 159-62 (1992).

18. Kobayashi, Y., Nakajima, T. & Inoue, I. Molecular modeling of the dimeric structure of human lipoprotein lipase and functional studies of the carboxyl-terminal domain. *European journal of biochemistry / FEBS* **269**, 4701-10 (2002).

19. Dugi, K.A., Dichek, H.L. & Santamarina-Fojo, S. Human hepatic and lipoprotein lipase: the loop covering the catalytic site mediates lipase substrate specificity. *J Biol Chem* **270**, 25396-401 (1995).

20. Dugi, K.A., Dichek, H.L., Talley, G.D., Brewer, H.B., Jr. & Santamarina-Fojo, S. Human lipoprotein lipase: the loop covering the catalytic site is essential for interaction with lipid substrates. *J Biol Chem* **267**, 25086-91 (1992).

21. Lookene, A., Groot, N.B., Kastelein, J.J., Olivecrona, G. & Bruin, T. Mutation of tryptophan residues in lipoprotein lipase. Effects on stability, immunoreactivity, and catalytic properties. *The Journal of biological chemistry* **272**, 766-72 (1997).

22. Roy, A., Xu, D., Poisson, J. & Zhang, Y. A protocol for computer-based protein structure and function prediction. *Journal of visualized experiments : JoVE*, e3259 (2011).

23. Biggerstaff, K.D. & Wooten, J.S. Understanding lipoproteins as transporters of cholesterol and other lipids. *Adv Physiol Educ* **28**, 105-6 (2004).

24. Williams, K.J. Molecular processes that handle -- and mishandle -- dietary lipids. *J Clin Invest* **118**, 3247-59 (2008).

25. Young, S.G. & Zechner, R. Biochemistry and pathophysiology of intravascular and intracellular lipolysis. *Genes Dev* **27**, 459-84 (2013).

26. Santamarina-Fojo, S. & Brewer, H.B., Jr. The familial hyperchylomicronemia syndrome. New insights into underlying genetic defects. *JAMA* **265**, 904-8 (1991).

27. Dichek, H.L. et al. Identification of two separate allelic mutations in the lipoprotein lipase gene of a patient with the familial hyperchylomicronemia syndrome. *J Biol Chem* **266**, 473-7 (1991).

28. Shimada, M. et al. Overexpression of human lipoprotein lipase in transgenic mice. Resistance to diet-induced hypertriglyceridemia and hypercholesterolemia. *J Biol Chem* **268**, 17924-9 (1993).

29. Connelly, P.W. & Hegele, R.A. Hepatic lipase deficiency. *Crit Rev Clin Lab Sci* **35**, 547-72 (1998).

30. Ishida, T. et al. Endothelial lipase is a major determinant of HDL level. *J Clin Invest* **111**, 347-55 (2003).

31. Kersten, S. Physiological regulation of lipoprotein lipase. *Biochim Biophys Acta* **1841**, 919-33 (2014).

32. Ramasamy, I. Update on the molecular biology of dyslipidemias. *Clin Chim Acta* **454**, 143-85 (2016).

33. LaRosa, J.C., Levy, R.I., Herbert, P., Lux, S.E. & Fredrickson, D.S. A specific apoprotein activator for lipoprotein lipase. *Biochem Biophys Res Commun* **41**, 57-62 (1970).

34. Breckenridge, W.C., Little, J.A., Steiner, G., Chow, A. & Poapst, M. Hypertriglyceridemia associated with deficiency of apolipoprotein C-II. *N Engl J Med* **298**, 1265-73 (1978).

35. Kei, A.A., Filippatos, T.D., Tsimihodimos, V. & Elisaf, M.S. A review of the role of apolipoprotein C-II in lipoprotein metabolism and cardiovascular disease. *Metabolism* **61**, 906-21 (2012).

36. McIlhargey, T.L., Yang, Y., Wong, H. & Hill, J.S. Identification of a lipoprotein lipase cofactor-binding site by chemical cross-linking and transfer of apolipoprotein C-II-responsive lipolysis from lipoprotein lipase to hepatic lipase. *J Biol Chem* **278**, 23027-35 (2003).

37. Jong, M.C., Hofker, M.H. & Havekes, L.M. Role of ApoCs in lipoprotein metabolism: functional differences between ApoC1, ApoC2, and ApoC3. *Arterioscler Thromb Vasc Biol* **19**, 472-84 (1999).

38. Berbee, J.F., van der Hoogt, C.C., Sundararaman, D., Havekes, L.M. & Rensen, P.C. Severe hypertriglyceridemia in human APOC1 transgenic mice is caused by apoC-I-induced inhibition of LPL. *J Lipid Res* **46**, 297-306 (2005).

39. Ito, Y., Azrolan, N., O'Connell, A., Walsh, A. & Breslow, J.L. Hypertriglyceridemia as a result of human apo CIII gene expression in transgenic mice. *Science* **249**, 790-3 (1990).

40. Jong, M.C. et al. Apolipoprotein C-III deficiency accelerates triglyceride hydrolysis by lipoprotein lipase in wild-type and apoE knockout mice. *J Lipid Res* **42**, 1578-85 (2001).

41. Pollin, T.I. et al. A null mutation in human APOC3 confers a favorable plasma lipid profile and apparent cardioprotection. *Science* **322**, 1702-5 (2008).

42. Tg et al. Loss-of-function mutations in APOC3, triglycerides, and coronary disease. *N Engl J Med* **371**, 22-31 (2014).

43. Jong, M.C. et al. Reversal of hyperlipidaemia in apolipoprotein C1 transgenic mice by adenovirus-mediated gene delivery of the low-density-lipoprotein receptor, but not by the very-low-density-lipoprotein receptor. *Biochem J* **338 (Pt 2)**, 281-7 (1999).

44. Larsson, M., Vorrsjo, E., Talmud, P., Lookene, A. & Olivecrona, G. Apolipoproteins C-I and C-III inhibit lipoprotein lipase activity by displacement of the enzyme from lipid droplets. *J Biol Chem* **288**, 33997-4008 (2013).

45. Calandra, S., Priore Oliva, C., Tarugi, P. & Bertolini, S. APOA5 and triglyceride metabolism, lesson from human APOA5 deficiency. *Curr Opin Lipidol* **17**, 122-7 (2006).

46. Pennacchio, L.A. & Rubin, E.M. Apolipoprotein A5, a newly identified gene that affects plasma triglyceride levels in humans and mice. *Arterioscler Thromb Vasc Biol* **23**, 529-34 (2003).

47. Marcais, C. et al. Apoa5 Q139X truncation predisposes to late-onset hyperchylomicronemia due to lipoprotein lipase impairment. *J Clin Invest* **115**, 2862-9 (2005).

48. Priore Oliva, C. et al. Inherited apolipoprotein A-V deficiency in severe hypertriglyceridemia. *Arterioscler Thromb Vasc Biol* **25**, 411-7 (2005).

49. Li, Y. & Teng, C. Angiopoietin-like proteins 3, 4 and 8: regulating lipid metabolism and providing new hope for metabolic syndrome. *J Drug Target* **22**, 679-87 (2014).

50. Lafferty, M.J., Bradford, K.C., Erie, D.A. & Neher, S.B. Angiopoietin-like protein 4 inhibition of lipoprotein lipase: evidence for reversible complex formation. *J Biol Chem* **288**, 28524-34 (2013).

51. Fu, Z., Yao, F., Abou-Samra, A.B. & Zhang, R. Lipasin, thermoregulated in brown fat, is a novel but atypical member of the angiopoietin-like protein family. *Biochem Biophys Res Commun* **430**, 1126-31 (2013).

52. Lee, E.C. et al. Identification of a new functional domain in angiopoietin-like 3 (ANGPTL3) and angiopoietin-like 4 (ANGPTL4) involved in binding and inhibition of lipoprotein lipase (LPL). *J Biol Chem* **284**, 13735-45 (2009).

53. Quagliarini, F. et al. Atypical angiopoietin-like protein that regulates ANGPTL3. *Proc Natl Acad Sci U S A* **109**, 19751-6 (2012).

54. Zhang, R. The ANGPTL3-4-8 model, a molecular mechanism for triglyceride trafficking. *Open Biol* **6**(2016).

55. Davies, B.S. et al. GPIHBP1 is responsible for the entry of lipoprotein lipase into capillaries. *Cell Metab* **12**, 42-52 (2010).

56. Beigneux, A.P. et al. Glycosylphosphatidylinositol-anchored high-density lipoprotein-binding protein 1 plays a critical role in the lipolytic processing of chylomicrons. *Cell Metab* **5**, 279-91 (2007).

57. Young, S.G. et al. GPIHBP1, an endothelial cell transporter for lipoprotein lipase. *Journal of lipid research* **52**, 1869-84 (2011).

58. Gin, P. et al. The acidic domain of GPIHBP1 is important for the binding of lipoprotein lipase and chylomicrons. *J Biol Chem* **283**, 29554-62 (2008).

59. Gin, P. et al. Binding preferences for GPIHBP1, a glycosylphosphatidylinositol-anchored protein of capillary endothelial cells. *Arterioscler Thromb Vasc Biol* **31**, 176-82 (2011).

60. Doolittle, M.H. & Peterfy, M. Mechanisms of lipase maturation. *Clinical lipidology* **5**, 71-85 (2010).

61. Wong, H. et al. A molecular biology-based approach to resolve the subunit orientation of lipoprotein lipase. *Proc Natl Acad Sci U S A* **94**, 5594-8 (1997).

62. Kobayashi, Y., Nakajima, T. & Inoue, I. Molecular modeling of the dimeric structure of human lipoprotein lipase and functional studies of the carboxyl-terminal domain. *Eur J Biochem* **269**, 4701-10 (2002).

63. Griffon, N. et al. Identification of the active form of endothelial lipase, a homodimer in a head-to-tail conformation. *J Biol Chem* **284**, 23322-30 (2009).

64. Hill, J.S., Davis, R.C., Yang, D., Schotz, M.C. & Wong, H. Hepatic lipase: high-level expression and subunit structure determination. *Methods Enzymol* **284**, 232-46 (1997).

65. Wong, H. & Schotz, M.C. The lipase gene family. *Journal of lipid research* **43**, 993-9 (2002).

66. Ben-Zeev, O., Mao, H.Z. & Doolittle, M.H. Maturation of lipoprotein lipase in the endoplasmic reticulum. Concurrent formation of functional dimers and inactive aggregates. *J Biol Chem* **277**, 10727-38 (2002).

67. Ben-Zeev, O. & Doolittle, M.H. Maturation of hepatic lipase. Formation of functional enzyme in the endoplasmic reticulum is the rate-limiting step in its secretion. *J Biol Chem* **279**, 6171-81 (2004).

68. Hebert, D.N., Garman, S.C. & Molinari, M. The glycan code of the endoplasmic reticulum: asparagine-linked carbohydrates as protein maturation and quality-control tags. *Trends Cell Biol* **15**, 364-70 (2005).

69. Kobayashi, J. et al. A naturally occurring mutation at the second base of codon asparagine 43 in the proposed N-linked glycosylation site of human lipoprotein lipase: in vivo evidence that asparagine 43 is essential for catalysis and secretion. *Biochem Biophys Res Commun* **205**, 506-15 (1994).

70. Ben-Zeev, O., Stahnke, G., Liu, G., Davis, R.C. & Doolittle, M.H. Lipoprotein lipase and hepatic lipase: the role of asparagine-linked glycosylation in the expression of a functional enzyme. *J Lipid Res* **35**, 1511-23 (1994).

71. Miller, G.C. et al. Role of N-linked glycosylation in the secretion and activity of endothelial lipase. *J Lipid Res* **45**, 2080-7 (2004).

72. Yang, C.Y. et al. Structure of bovine milk lipoprotein lipase. *J Biol Chem* **264**, 16822-7 (1989).

73. Lo, J.Y., Smith, L.C. & Chan, L. Lipoprotein lipase: role of intramolecular disulfide bonds in enzyme catalysis. *Biochem Biophys Res Commun* **206**, 266-71 (1995).

74. van Tilbeurgh, H., Roussel, A., Lalouel, J.M. & Cambillau, C. Lipoprotein lipase. Molecular model based on the pancreatic lipase x-ray structure: consequences for heparin binding and catalysis. *J Biol Chem* **269**, 4626-33 (1994).

75. Voss, C.V. et al. Mutations in lipoprotein lipase that block binding to the endothelial cell transporter GPIHBP1. *Proceedings of the National Academy of Sciences of the United States of America* **108**, 7980-4 (2011).

76. Henderson, H.E., Hassan, F., Marais, D. & Hayden, M.R. A new mutation destroying disulphide bridging in the C-terminal domain of lipoprotein lipase. *Biochem Biophys Res Commun* **227**, 189-94 (1996).

77. Paterniti, J.R., Jr., Brown, W.V., Ginsberg, H.N. & Artzt, K. Combined lipase deficiency (cld): a lethal mutation on chromosome 17 of the mouse. *Science* **221**, 167-9 (1983).

78. Davis, R.C., Ben-Zeev, O., Martin, D. & Doolittle, M.H. Combined lipase deficiency in the mouse. Evidence of impaired lipase processing and secretion. *The Journal of biological chemistry* **265**, 17960-6 (1990).

79. Freeze, H.H. & Kranz, C. Endoglycosidase and glycoamidase release of N-linked glycans. *Curr Protoc Protein Sci* **Chapter 12**, Unit12 4 (2010).

80. Peterfy, M., Mao, H.Z. & Doolittle, M.H. The cld mutation: narrowing the critical chromosomal region and selecting candidate genes. *Mamm Genome* **17**, 1013-24 (2006).

81. Peterfy, M. et al. Mutations in LMF1 cause combined lipase deficiency and severe hypertriglyceridemia. *Nat Genet* **39**, 1483-7 (2007).

82. Doolittle, M.H. et al. Lipase maturation factor LMF1, membrane topology and interaction with lipase proteins in the endoplasmic reticulum. *The Journal of biological chemistry* **284**, 33623-33 (2009).

83. Briquet-Laugier, V., Ben-Zeev, O., White, A. & Doolittle, M.H. cld and lec23 are disparate mutations that affect maturation of lipoprotein lipase in the endoplasmic reticulum. *J Lipid Res* **40**, 2044-58 (1999).

84. Cefalu, A.B. et al. Novel LMF1 nonsense mutation in a patient with severe hypertriglyceridemia. *J Clin Endocrinol Metab* **94**, 4584-90 (2009).

85. Coleman, T. et al. COOH-terminal disruption of lipoprotein lipase in mice is lethal in homozygotes, but heterozygotes have elevated triglycerides and impaired enzyme activity. *J Biol Chem* **270**, 12518-25 (1995).

86. Ehrhardt, N., Bedoya, C. & Peterfy, M. Embryonic viability, lipase deficiency, hypertriglyceridemia and neonatal lethality in a novel LMF1-deficient mouse model. *Nutr Metab (Lond)* **11**, 37 (2014).

87. Durrington, P. Dyslipidaemia. *Lancet* **362**, 717-31 (2003).

88. Merkel, M., Eckel, R.H. & Goldberg, I.J. Lipoprotein lipase: genetics, lipid uptake, and regulation. *J Lipid Res* **43**, 1997-2006 (2002).

89. Surendran, R.P. et al. Mutations in LPL, APOC2, APOA5, GPIHBP1 and LMF1 in patients with severe hypertriglyceridaemia. *Journal of internal medicine* (2012).

90. Santamarina-Fojo, S. & Brewer, H.B., Jr. Lipoprotein lipase: structure, function and mechanism of action. *Int J Clin Lab Res* **24**, 143-7 (1994).

91. Wittrup, H.H., Tybjaerg-Hansen, A. & Nordestgaard, B.G. Lipoprotein lipase mutations, plasma lipids and lipoproteins, and risk of ischemic heart disease. A meta-analysis. *Circulation* **99**, 2901-7 (1999).

92. Hokanson, J.E. Functional variants in the lipoprotein lipase gene and risk cardiovascular disease. *Curr Opin Lipidol* **10**, 393-9 (1999).

93. Grundy, S.M. The issue of statin safety: where do we stand? *Circulation* **111**, 3016-9 (2005).

94. Werner, C. et al. Risk prediction with triglycerides in patients with stable coronary disease on statin treatment. *Clin Res Cardiol* (2014).

95. Staels, B. et al. Mechanism of action of fibrates on lipid and lipoprotein metabolism. *Circulation* **98**, 2088-93 (1998).

96. Stroes, E.S. et al. Intramuscular administration of AAV1-lipoprotein lipase S447X lowers triglycerides in lipoprotein lipase-deficient patients. *Arterioscler Thromb Vasc Biol* **28**, 2303-4 (2008).

97. Gaudet, D. et al. Efficacy and long-term safety of alipogene tiparvovec (AAV1-LPLS447X) gene therapy for lipoprotein lipase deficiency: an open-label trial. *Gene Ther* **20**, 361-9 (2013).

98. Han, X. & Ni, W. Cost-Effectiveness Analysis of Glybera for The Treatment of Lipoprotein Lipase Deficiency. *Value Health* **18**, A756 (2015).

99. Do, R. et al. Common variants associated with plasma triglycerides and risk for coronary artery disease. *Nat Genet* **45**, 1345-52 (2013).

100. Miller, M. et al. Triglycerides and cardiovascular disease: a scientific statement from the American Heart Association. *Circulation* **123**, 2292-333 (2011).

101. Fan, J.Q. A counterintuitive approach to treat enzyme deficiencies: use of enzyme inhibitors for restoring mutant enzyme activity. *Biological chemistry* **389**, 1-11 (2008).

102. Khanna, R. et al. The pharmacological chaperone 1-deoxygalactonojirimycin reduces tissue globotriaosylceramide levels in a mouse model of Fabry disease.

Molecular therapy : the journal of the American Society of Gene Therapy **18**, 23-33 (2010).

103. Hegele, R.A. & Pollex, R.L. Hypertriglyceridemia: phenomics and genomics. *Mol Cell Biochem* (2009).

104. Cefalu, A.B. et al. Novel LMF1 nonsense mutation in a patient with severe hypertriglyceridemia. *The Journal of clinical endocrinology and metabolism* **94**, 4584-90 (2009).

105. Warden, C.H. et al. Chromosomal localization of lipolytic enzymes in the mouse: pancreatic lipase, colipase, hormone-sensitive lipase, hepatic lipase, and carboxyl ester lipase. *J Lipid Res* **34**, 1451-5 (1993).

106. Olivecrona, T., Chernick, S.S., Bengtsson-Olivecrona, G., Garrison, M. & Scow, R.O. Synthesis and secretion of lipoprotein lipase in 3T3-L1 adipocytes. Demonstration of inactive forms of lipase in cells. *J Biol Chem* **262**, 10748-59 (1987).

107. Ivanov, A.I. *Exocytosis and endocytosis*, xv, 412 p. (Humana Press, Totowa, N.J., 2008).

108. Li, H., Korennykh, A.V., Behrman, S.L. & Walter, P. Mammalian endoplasmic reticulum stress sensor IRE1 signals by dynamic clustering. *Proceedings of the National Academy of Sciences of the United States of America* **107**, 16113-8 (2010).

109. Schutze, M.P., Peterson, P.A. & Jackson, M.R. An N-terminal double-arginine motif maintains type II membrane proteins in the endoplasmic reticulum. *The EMBO journal* **13**, 1696-705 (1994).

110. Boedeker, J.C., Doolittle, M.H. & White, A.L. Differential effect of combined lipase deficiency (cld/cld) on human hepatic lipase and lipoprotein lipase secretion. *J Lipid Res* **42**, 1858-64 (2001).

111. Lorenz, H., Hailey, D.W., Wunder, C. & Lippincott-Schwartz, J. The fluorescence protease protection (FPP) assay to determine protein localization and membrane topology. *Nat Protoc* **1**, 276-9 (2006).

112. Walker, J.M. *The protein protocols handbook*, xxiv, 1146 p. (Humana Press, Totowa, N.J., 2002).

113. Ben-Zeev, O., Mao, H.Z. & Doolittle, M.H. Maturation of lipoprotein lipase in the endoplasmic reticulum. Concurrent formation of functional dimers and inactive aggregates. *The Journal of biological chemistry* **277**, 10727-38 (2002).

114. Schwanhausser, B. et al. Corrigendum: Global quantification of mammalian gene expression control. *Nature* **495**, 126-7 (2013).

115. Schwanhausser, B. et al. Global quantification of mammalian gene expression control. *Nature* **473**, 337-42 (2011).

116. Masuno, H., Blanchette-Mackie, E.J., Chernick, S.S. & Scow, R.O. Synthesis of inactive nonsecretable high mannose-type lipoprotein lipase by cultured brown adipocytes of combined lipase-deficient cld/cld mice. *The Journal of biological chemistry* **265**, 1628-38 (1990).

117. Doolittle, M. et al. Lipase maturation factor 1 (Lmf1): Membrane topology and interaction with lipase proteins in the endoplasmic reticulum. *J Biol Chem* (2009).

118. Babilonia-Rosa, M. & Neher, S.B. Purification, Cellular Levels, and Functional Domains of LMF1. *Biochemical and biophysical research communications* (2014).

119. Riemer, J., Bulleid, N. & Herrmann, J.M. Disulfide formation in the ER and mitochondria: two solutions to a common process. *Science* **324**, 1284-7 (2009).

120. Chakravarthi, S., Jessop, C.E. & Bulleid, N.J. The role of glutathione in disulphide bond formation and endoplasmic-reticulum-generated oxidative stress. *EMBO Rep* **7**, 271-5 (2006).

121. Berkmen, M., Boyd, D. & Beckwith, J. The nonconsecutive disulfide bond of Escherichia coli phytase (AppA) renders it dependent on the protein-disulfide isomerase, DsbC. *J Biol Chem* **280**, 11387-94 (2005).

122. Ito, K. & Inaba, K. The disulfide bond formation (Dsb) system. *Curr Opin Struct Biol* **18**, 450-8 (2008).

123. Babilonia-Rosa, M.A. & Neher, S.B. Purification, cellular levels, and functional domains of lipase maturation factor 1. *Biochem Biophys Res Commun* (2014).

124. Edelheit, O., Hanukoglu, A. & Hanukoglu, I. Simple and efficient site-directed mutagenesis using two single-primer reactions in parallel to generate mutants for protein structure-function studies. *BMC Biotechnol* **9**, 61 (2009).

125. Liu, W., Brock, A., Chen, S., Chen, S. & Schultz, P.G. Genetic incorporation of unnatural amino acids into proteins in mammalian cells. *Nat Methods* **4**, 239-44 (2007).

126. Heckman, K.L. & Pease, L.R. Gene splicing and mutagenesis by PCR-driven overlap extension. *Nature protocols* **2**, 924-32 (2007).

127. Ranaldi, S. et al. Amplitude of pancreatic lipase lid opening in solution and identification of spin label conformational subensembles by combining continuous wave and pulsed EPR spectroscopy and molecular dynamics. *Biochemistry* **49**, 2140-9 (2010).

128. Liu, C.C. & Schultz, P.G. Adding new chemistries to the genetic code. *Annual review of biochemistry* **79**, 413-44 (2010).

129. Chin, J.W., Martin, A.B., King, D.S., Wang, L. & Schultz, P.G. Addition of a photocrosslinking amino acid to the genetic code of Escherichiacoli. *Proceedings of the National Academy of Sciences of the United States of America* **99**, 11020-4 (2002).

130. Liu, W., Brock, A., Chen, S. & Schultz, P.G. Genetic incorporation of unnatural amino acids into proteins in mammalian cells. *Nature methods* **4**, 239-44 (2007).

131. Sha, H. et al. The ER-associated degradation adaptor protein Sel1L regulates LPL secretion and lipid metabolism. *Cell metabolism* **20**, 458-70 (2014).

132. Doolittle, M.H. et al. Hepatic lipase maturation: a partial proteome of interacting factors. *J Lipid Res* **50**, 1173-84 (2009).

133. Kozlov, G., Maattanen, P., Thomas, D.Y. & Gehring, K. A structural overview of the PDI family of proteins. *FEBS J* **277**, 3924-36 (2010).

134. Galligan, J.J. & Petersen, D.R. The human protein disulfide isomerase gene family. *Hum Genomics* **6**, 6 (2012).

135. Wang, C.C. & Tsou, C.L. Protein disulfide isomerase is both an enzyme and a chaperone. *FASEB J* **7**, 1515-7 (1993).

136. Cai, H., Wang, C.C. & Tsou, C.L. Chaperone-like activity of protein disulfide isomerase in the refolding of a protein with no disulfide bonds. *J Biol Chem* **269**, 24550-2 (1994).

137. Wang, Z.V. et al. Secretion of the adipocyte-specific secretory protein adiponectin critically depends on thiol-mediated protein retention. *Mol Cell Biol* **27**, 3716-31 (2007).

138. Cortini, M. & Sitia, R. From antibodies to adiponectin: role of ERp44 in sizing and timing protein secretion. *Diabetes, obesity & metabolism* **12 Suppl 2**, 39-47 (2010).

139. Rutkevich, L.A., Cohen-Doyle, M.F., Brockmeier, U. & Williams, D.B. Functional relationship between protein disulfide isomerase family members during the

oxidative folding of human secretory proteins. *Molecular biology of the cell* **21**, 3093-105 (2010).

140. Jessop, C.E., Watkins, R.H., Simmons, J.J., Tasab, M. & Bulleid, N.J. Protein disulphide isomerase family members show distinct substrate specificity: P5 is targeted to BiP client proteins. *Journal of cell science* **122**, 4287-95 (2009).

141. Oka, O.B., Pringle, M.A., Schopp, I.M., Braakman, I. & Bulleid, N.J. ERdj5 is the ER reductase that catalyzes the removal of non-native disulfides and correct folding of the LDL receptor. *Molecular cell* **50**, 793-804 (2013).

142. Ushioda, R. et al. ERdj5 is required as a disulfide reductase for degradation of misfolded proteins in the ER. *Science* **321**, 569-72 (2008).

143. Arnold, S.M., Fessler, L.I., Fessler, J.H. & Kaufman, R.J. Two homologues encoding human UDP-glucose:glycoprotein glucosyltransferase differ in mRNA expression and enzymatic activity. *Biochemistry* **39**, 2149-63 (2000).

144. Patwari, P., Higgins, L.J., Chutkow, W.A., Yoshioka, J. & Lee, R.T. The interaction of thioredoxin with Txnip. Evidence for formation of a mixed disulfide by disulfide exchange. *The Journal of biological chemistry* **281**, 21884-91 (2006).

145. Meister, A. Selective modification of glutathione metabolism. *Science* **220**, 472-7 (1983).

146. Wang, H. et al. Tunicamycin-induced unfolded protein response in the developing mouse brain. *Toxicol Appl Pharmacol* **283**, 157-67 (2015).

147. Hampe, L. et al. Regulation and Quality Control of Adiponectin Assembly by Endoplasmic Reticulum Chaperone ERp44. *The Journal of biological chemistry* **290**, 18111-23 (2015).

148. Vavassori, S. et al. A pH-regulated quality control cycle for surveillance of secretory protein assembly. *Molecular cell* **50**, 783-92 (2013).

149. Hagiwara, M. et al. Structural basis of an ERAD pathway mediated by the ER-resident protein disulfide reductase ERdj5. *Molecular cell* **41**, 432-44 (2011).

150. Kojer, K. & Riemer, J. Balancing oxidative protein folding: the influences of reducing pathways on disulfide bond formation. *Biochimica et biophysica acta* **1844**, 1383-90 (2014).

151. Tsunoda, S. et al. Intact protein folding in the glutathione-depleted endoplasmic reticulum implicates alternative protein thiol reductants. *eLife* **3**, e03421 (2014).

152. Finn, R.D. et al. Pfam: the protein families database. *Nucleic acids research* **42**, D222-30 (2014).

153. Muller, F.H. et al. Coupling of the pathway of sulphur oxidation to dioxygen reduction: characterization of a novel membrane-bound thiosulphate:quinone oxidoreductase. *Molecular microbiology* **53**, 1147-60 (2004).

154. Nambi, S. et al. The Oxidative Stress Network of Mycobacterium tuberculosis Reveals Coordination between Radical Detoxification Systems. *Cell host & microbe* **17**, 829-37 (2015).

155. van der Palen, C.J., Reijnders, W.N., de Vries, S., Duine, J.A. & van Spanning, R.J. MauE and MauD proteins are essential in methylamine metabolism of Paracoccus denitrificans. *Antonie van Leeuwenhoek* **72**, 219-28 (1997).

156. Jessop, C.E., Tavender, T.J., Watkins, R.H., Chambers, J.E. & Bulleid, N.J. Substrate specificity of the oxidoreductase ERp57 is determined primarily by its interaction with calnexin and calreticulin. *The Journal of biological chemistry* **284**, 2194-202 (2009).

157. Arnold, S.M. & Kaufman, R.J. The noncatalytic portion of human UDP-glucose: glycoprotein glucosyltransferase I confers UDP-glucose binding and transferase function to the catalytic domain. *The Journal of biological chemistry* **278**, 43320-8 (2003).

158. Takeda, Y. et al. Both isoforms of human UDP-glucose:glycoprotein glucosyltransferase are enzymatically active. *Glycobiology* **24**, 344-50 (2014).

159. Buzzi, L.I., Simonetta, S.H., Parodi, A.J. & Castro, O.A. The two Caenorhabditis elegans UDP-glucose:glycoprotein glucosyltransferase homologues have distinct biological functions. *PloS one* **6**, e27025 (2011).

160. Anelli, T. et al. Thiol-mediated protein retention in the endoplasmic reticulum: the role of ERp44. *EMBO J* **22**, 5015-22 (2003).

161. Zhang, B. et al. Combined deficiency of factor V and factor VIII is due to mutations in either LMAN1 or MCFD2. *Blood* **107**, 1903-7 (2006).

162. Hughes, H. et al. Organisation of human ER-exit sites: requirements for the localisation of Sec16 to transitional ER. *J Cell Sci* **122**, 2924-34 (2009).

163. Cho, S.H. & Beckwith, J. Mutations of the membrane-bound disulfide reductase DsbD that block electron transfer steps from cytoplasm to periplasm in Escherichia coli. *J Bacteriol* **188**, 5066-76 (2006).

164. Cho, S.H., Porat, A., Ye, J. & Beckwith, J. Redox-active cysteines of a membrane electron transporter DsbD show dual compartment accessibility. *EMBO J* **26**, 3509-20 (2007).

165. Babilonia-Rosa, M.A. & Neher, S.B. Purification, cellular levels, and functional domains of lipase maturation factor 1. *Biochem Biophys Res Commun* **450**, 423-8 (2014).

166. Borch, J. & Hamann, T. The nanodisc: a novel tool for membrane protein studies. *Biol Chem* **390**, 805-14 (2009).

167. Bayburt, T.H. & Sligar, S.G. Membrane protein assembly into Nanodiscs. *FEBS Lett* **584**, 1721-7 (2010).

168. Bengtsson-Olivecrona, G. & Olivecrona, T. Phospholipase activity of milk lipoprotein lipase. *Methods Enzymol* **197**, 345-56 (1991).

169. Basu, D., Manjur, J. & Jin, W. Determination of lipoprotein lipase activity using a novel fluorescent lipase assay. *Journal of lipid research* **52**, 826-32 (2011).

170. Katzen, F. & Beckwith, J. Transmembrane electron transfer by the membrane protein DsbD occurs via a disulfide bond cascade. *Cell* **103**, 769-79 (2000).